IZMİR KATIP CELEBI UNIVERSITY ★ GRADUATE SCHOOL OF NATURAL AND APPLIED SCIENCES

DEVELOPMENT, PRODUCTION AND CHARACTERIZATION OF CERAMIC BASED 3D TISSUE SCAFFOLDS

M.Sc. THESIS

Betül ALDEMİR

Department of Biomedical Technologies

Thesis Advisor: Assistant Professor Hakan OFLAZ

Co-Advisor: Assistant Professor Ozan KARAMAN

MARCH, 2016

IZMİR KATIP CELEBI UNIVERSITY ★ GRADUATE SCHOOL OF NATURAL AND APPLIED SCIENCES

DEVELOPMENT, PRODUCTION AND CHARACTERIZATION OF CERAMIC BASED 3D TISSUE SCAFFOLDS

M.Sc. THESIS

Betül ALDEMİR

Y130101025

Department of Biomedical Technologies

Thesis Advisor: Assistant Professor Hakan OFLAZ

Co-Advisor: Assistant Professor Ozan KARAMAN

MARCH, 2016

İZMİR KÂTİP ÇELEBİ ÜNİVERSİTESİ ★ FEN BİLİMLERİ ENSTİTÜSÜ

SERAMİK TABANLI 3B DOKU İSKELELERİNİN GELİŞTİRİLİP, ÜRETİLMESİ VE KARAKTERİZASYONU

YÜKSEK LİSANS TEZİ

Betül ALDEMİR

(Y130101025)

Biyomedikal Teknolojileri Anabilim Dalı

Tez Danışmanı: Yrd. Doç. Dr. Hakan OFLAZ

Eş Danışman: Yrd. Doç. Dr. Ozan KARAMAN

MART, 2016

Betül Aldemir, a **M.Sc.** student of **IZMIR KATIP CELEBI UNIVERSITY Institute of Graduate School of Natural and Applied Science** student ID **Y130101025** successfully defended the **thesis** entitled **DEVELOPMENT, PRODUCTION AND CHARACTERIZATION OF CERAMIC BASED 3D TISSUE SCAFFOLDS** which she prepared after fulfilling the requirements specified in the associated legislations, before the jury whose signatures are below.

Thesis Advisor : Assist. Prof. Dr. Hakan OFLAZ .....

Jury Members : Prof. Dr. Adnan KAYA .....

Assist. Prof. Dr.Mehmet SARIKANAT .....

Date of Submission : February 2016

Date of Defense : 26 February 2016

To my lovely family;

Serkan Dikici, Nurten Aldemir, Ozan Aldemir, Metin Aldemir.

You mean the world to me.

FOREWORD

This thesis would not have been possible without the support of many to whom I express my sincere gratitude.

Before anything else, I would like to express my deepest heartfelt gratitude to Dear Dr. Hakan Oflaz for his guidance and encouragement about my scientific interest. In addition, I am very appreciated for trusting me for design issues and creating a chance for me to combine my occupation and design passion.

I am very glad to be the closest witness to evolution of four wall into tissue engineering laboratory. I would like to thank to dear Dr. Hakan Oflaz and Dr. Ozan Karaman for giving this opportunity to me. I am grateful to my co-supervisor Dr. Karaman who enrich my vision about tissue engineering with his valuable lectures and personal conversations.

I would like to thank my previous supervisor at the University of Ege, Dr. Aylin Şendemir Ürkmez for transmitting me her enthusiasm and passion for biomaterials and tissue engineering. Furthermore, I am grateful to her for introducing me to Dr. Oflaz.

Let me express my sincere thanks to Dr. Mehmet Sarıkanat for his helps about data interpretation for T_G and T_M analysis. Also, I would like to thanks to him and Dr. Adnan Kaya to be included in my MSc adventure as a member of jury committee.

I am very thankful to Savaş Öztürk who helps me for sintering processes. My lovely thank goes to dear colleagues Afra Demirci, Ziyşan Yaralı and Hakkı Köse for their support and best wishes. I would like to thank undergraduate student Emine Kahraman for aiding me in cell culture laboratory.

I am very glad to meet with Budin Akarca Ind. Trade. Ltd. and its big hearted employees. I am so appreciated for their help for homogenization processes. I would like to acknowledge HGO Medikal Ind. Trade. Inc. for supporting the research in design, production, analysis and consultancy issues.

My warmest gratitude for my lovely mother Nurten Aldemir and my father, and also my first teacher Metin Aldemir who are always supporting and encouraging me with their best wishes, none of this would have been possible without their love and patience. I also thank to my first friend, dearie brother Ozan Aldemir for his endless support throughout my life.

I owe my deepest gratitude to my dear fiancé, friend and companion Serkan Dikici. Without his support, understanding, patience and everlasting love, I could not have succeeded in this. He is the shareholder of my professional and personal life.

I would like to thank to Scientific and Technological Research Council of Turkey (TUBİTAK, and the University of Izmir Kâtip Çelebi, Department of Scientific Research Projects (BAP) for financing the research.

February, 2016 **Betül ALDEMİR**

TABLE OF CONTENTS

ABBREVIATIONS

2D	**:**	Two Dimensional
3D	**:**	Three Dimensional
3DP	**:**	3D Printing
ALP	**:**	Alkaline Phosphatase
AM	**:**	Additive Manufacturing
BMSC	**:**	Bone Marrow Stem Cell
BTE	**:**	Bone Tissue Engineering
CaP	**:**	Calcium Phosphates
CAD	**:**	Computer Aided Design
CATE	**:**	Computer Aided Tissue Engineering
CS	**:**	Calcium Sulfate
CSHH	**:**	Calcium Sulfate Hemihydrate
CT	**:**	Computer-aided Tomography
DI	**:**	Deionized
DMEM	**:**	Dulbecco's Modified Eagle's Medium
DMSO	**:**	Dimethylsulfoxide
ECM	**:**	Extracellular Matrix
FBS	**:**	Fetal Bovine Serum
FDA	**:**	Food and Drug Administration
FDM	**:**	Fused Deposition Modelling
GH	**:**	Growth Hormone
HA	**:**	Hydroxyapatite
IGF	**:**	Insulin-like Growth Factor
LOM	**:**	Laminated Object Manufacturing
MRI	**:**	Magnetic Resonance Imaging
OBs	**:**	Osteoblasts
OCs	**:**	Osteoclasts
PBS	**:**	Phosphate Buffer Solution
RP	**:**	Rapid Prototyping
SBF	**:**	Simulated Body Fluid

SEM	**:**	Scanning Electron Microscopy
SFF, FFF	**:**	(Solid) Free Form Fabrication
SL, SLA	**:**	Stereolithography
SLS	**:**	Selective Laser Sintering
SS	**:**	Stainless Steel
STL	**:**	Surface Tessellation Language, Stereolithography
TCP	**:**	Tricalcium Phosphates
TE	**:**	Tissue Engineering
XRD	**:**	X-ray Diffraction

LIST OF TABLES

LIST OF FIGURES

DEVELOPMENT, PRODUCTION AND CHARACTERIZATION OF CERAMIC BASED 3D TISSUE SCAFFOLDS

SUMMARY

Production of defect-matching scaffolds is the most critical step in custom artificial bone applications. Three dimensional (3D) printing is one of the best techniques particularly for custom designs on artificial bone applications because of the high controllability and design independency. In this study, we aimed to develop, produce and characterize zinc doped ceramic based 3D printed scaffolds (calcium sulfate (CS) based) in an attempt to satisfy requirements of bone tissue engineering.

3D designed scaffolds were manufactured by using 3D printer. Zinc oxide doped and pure CS based scaffold groups were investigated by XRD, contact angle meter and SEM to be characterized. Then, mechanical properties were assessed by compression test. Cell viability of bone marrow stem cells (BMSCs) on printed scaffolds was determined by using MTT and cell attachment abilities were investigated by using SEM. The effects of the incorporation of zinc oxide in the commercial powder (CS) to mechanical and biological properties of the material were studied.

According to XRD results calcium sulfate hemihydrate (CSHH) powder was transformed into gypsum after printing process due to water content of binder. Following that gypsum was transform into anhydrite after sintering process due to water loss. Contact angle measurements showed that CS has a super hydrophilic character which supports cell attachment. It can be concluded that zinc addition increase both mechanical strength of CSHH samples and cell viability of BMSCs on CSHH based scaffolds. Similarly, cells attached properly and flattened on each group according to SEM micrographs. As a result, 0.5 wt% zinc doped samples have the best mechanical and biological properties among control, 0.1 wt%, 0.3 wt% and 0.5 wt% zinc doped groups.

Our long-term aim is to implant a custom artificial bone that is cultured with patient's own mesenchymal stem cells after determining defect architecture on patient's bone by using CT and printing that defect-matching 3D scaffold with appropriate non-toxic materials. Thus, in the scope of thesis, the optimum material composition was researched for current 3D printer in our laboratory.

SERAMİK TABANLI 3B DOKU İSKELELERİNİN GELİŞTİRİLİP, ÜRETİLMESİ VE KARAKTERİZASYONU

ÖZET

Defekte uygun doku iskelesi üretimi kişiye özel yapay kemik uygulamalarında en kritik basamağı oluşturmaktadır. Üç boyutlu (3B) yazdırma özellikle kişiye özel uygulamalarda iç ve dış tasarımın yüksek kontrol edilebilirliği ile en iyi üretim tekniklerinden biridir. Bu çalışma kapsamında kemik doku mühendisliğine iyi bir alternatif oluşturmak üzere çinko katkılı, seramik temelli (kalsiyum sülfat (KS)) doku iskelelerinin 3B yazdırma ile geliştirilip üretilmesi ve karakterizasyon testlerinin yapılması amaçlanmıştır.

3B tasarlanan iskeleler 3B yazıcı ile üretilmiştir. Çinko katkılı ve katkısız KS içerikli iskele grupları XRD, temas açısı ve SEM analizleri ile karakterize edilmiştir. Mekanik özellikleri basma testi yapılarak değerlendirilmiştir. Hücre canlılığı, MTT testi ile hücrelerin yüzeye tutunma yeteneği ise SEM gözlemleri ile belirlenmiştir. XRD analizi 3B yazıcının ticari tozu olan kalsiyum sülfat hemihidratın (KSHH), yapıştırıcı solüsyonun (binder) yüksek su içeriği nedeniyle yazdırma işlemi sonrası gypsuma dönüşmüş olduğunu, sinterleme işlemi sonunda ise su kaybı nedeni ile anhidrit formuna dönüşmüş olduğunu göstermektedir. Temas açı ölçümleri KSHH'ın hidrofilik karakterde olduğu ve ayrıca çinko ilavesinin KSHH örneklerin mekanik özelliklerini ve BMSC hücre hattının KSHH örnekler üzerindeki canlılığını olumlu yönde etkilediği görülmüştür. Benzer şekilde, SEM görüntülerinde görüldüğü üzere hücreler yüzeyde yassılaşarak oldukça iyi bir tutunma göstermektedirler. Sonuç olarak %0.5 çinko katkılı örneklerin kontrol, %0.1, %0.3 ve %0.5 çinko katkılı gruplar arasında en yüksek mekanik dayanıma sahip olduğu ve hücre canlılığı üzerindeki pozitif etkisinin de en fazla olduğu görülmüştür.

Çalışmanın uzun vadedeki amacı, CT görüntüleme ile defekt bölgesinin belirlenmesinin ardından, hastanın kendi mezenşimal hücreleri ekildiği defekte uygun doku iskelesinin, toksik olmayan, kemiğin mekanik ve biyolojik özelliklerini sağlayan malzeme kullanılarak üretimi ile kişiye özgü doku mühendisliği alanına katkı sağlamaktır. Tez kapsamında laboratuvarımızda bulunan 3B yazıcı ile üretilebilecek doku iskeleleri için optimum malzeme kompozisyonu araştırılmıştır.

1. INTRODUCTION

Many different bone diseases such as bone infections, fractures and osteoporosis are more frequently seen due to the rise in the average age of population or traumatic reasons (Bose, Roy, & Bandyopadhyay 2012; Rauh, Milan, Gunther, & Stiehler 2011). Since bone cannot manage to heal itself when a defect exceeds critical size, autographs or allographs are used for bone reconstruction in order to improve bone healing (Brydone, Meek, & Maclaine 2010; Lichte, Pape, Pufe, Kobbe, & Fischer 2011). Although four million bone grafting are performed in the world annually, autographs and allographs have significant limitations and risks such as donor site morbidity, high infection risk and immune response (Brydone et al. 2010; Inzana et al. 2014). At this point, bone tissue engineering (BTE) offers various strategies with biocompatible and well-designed 3D bone scaffolds to lead tissue formation (Subia 2010).

Many different biomaterials such as metals, polymers, ceramics and composites are used in BTE for scaffold production. Since ceramics are the main components of inorganic part of natural bone, ceramic based scaffolds are mostly used in BTE applications. Mostly preferred ceramic based materials for BTE are calcium phosphates (CaP), bioglass and calcium sulphate (CS) (Paul & Sharma 2007).

In our study CS which is a biocompatible and resorbable ceramic was used. CS also releases calcium ions which may provide an advantage for osteoblast formation (Thomas, Puleo, & Al-Sabbagh 2005). This biomaterial has been used in bone regeneration more than 100 years (Pietrzak & Ronk 2000; Thomas et al. 2005; Wu et al. 2012). Although this inexpensive medical grade resorbable CS has a long history in orthopaedics, powder based 3 dimensional (3D) printing technique brings innovation to its usage in tissue engineering (al Ruhaimi 2001).

In 3D printing technique, one thin layer of powder material is dispersed on a platform, following that the binder is sprayed onto the laid powder layer. The binder binds the powders to form a single 2 dimensional (2D) layer, therefore a sliced 2D

profile of a computer model is created. This process occurs many times to fabricate a 3D structure layer by layer until the whole model is completed (Lichte et al. 2011). 3DP can produce models that are difficult to create by conventional manufacturing methods (Utela, Storti, Anderson, & Ganter 2008). 3D printing is a versatile method and also have broad range of material for production. In addition to all, this method enables to design inner (porosity) and outer (border line) architecture of scaffolds. Due to its design independency, 3D printed CS products may be used in customized artificial bone grafts.

The main aim in personalized bone substitutes is to produce defect-matching scaffolds. There are certain essential steps for production of patient specific implants or grafts. Firstly, 3D model of defect side should be captured by CT scan and imported to the program. If the defect side has a healthy mirror image on body (such as deficient right hand, healthy left hand), CT data of the healthy area is captured to be used as a scaffold model. Otherwise, this model should be created by CAD (Computer Aided Design) software such as Solidworks or Inventor. After designing the inner architecture (flat or porous) and outer shape of the scaffold or implant, model is produced slice by slice by convenient additive manufacturing technique according to material type. Finally, patient specific model is sterilized and stem cells are isolated from human body to inoculate on 3D scaffolds.

In the scope of this thesis firstly, the commercial powder of Projet 160 3D printer was characterized by using XRD. Following that, zinc oxide which is one of the most important trace elements in human body and known to aid cell proliferation, differentiation, regulation of DNA synthesis, enzymatic functions and also has an positive effect on bone formation (Alhava, Olkkonen, Puittinen, & Nokso-Koivisto 1977; MacDonald 2000; Paul & Sharma 2007) was added at varying concentrations (control, 0.1 wt%, 0.3 wt% and 0.5 wt% Zn) to commercial printer powder to increase both the mechanical and biological properties of the samples which designed and manufactured by using 3D printing technology. Although all experiments were conducted on non-porous block samples, porous scaffolds with different porosities are produced to check the solubility and to optimize the pore size and intensity as a preliminary research for future study.

The aim of this study was combining the advantages of CS, zinc and 3D printing technique to investigate the usage potential of 3D printed, zinc doped CS samples as customized, bioresorbable bone grafts by using various disciplines such as material science, scaffold design and architecture, cell culture, and biomechanics. The main specific objectives are;

- Characterize the commercial powder of Projet 160 3D printer by using XRD before and after printing and after sintering processes.
- Study the effect of the incorporation of zinc oxide in the commercial powder (CS) to mechanical and biological properties of the material.
- The design, fabrication and characterization of the 3D block and porous scaffolds fabricated by 3D printing.
- Evaluation of zinc doped commercial powder for personalized scaffold fabrication processes.

2. LITERATURE REVIEW

2.1. Biology of Bone

2.1.1. Bone anatomy and physiology

Bone (osseous tissue), primary organ of skeletal system, supports the body, protects internal organs, produces blood cells, stores minerals and serves as a point of attachment for skeletal muscles. Besides its all these vital roles, osseous tissue is a highly complex system in terms of anatomy and physiology (Wang 2004). An adult human body is composed of average 206 bones (Bandyopadhyay 2006). They have varied structures in terms of shape, length, mechanical, biological and chemical properties (Rho, Kuhn-Spearing, & Zioupos 1998).

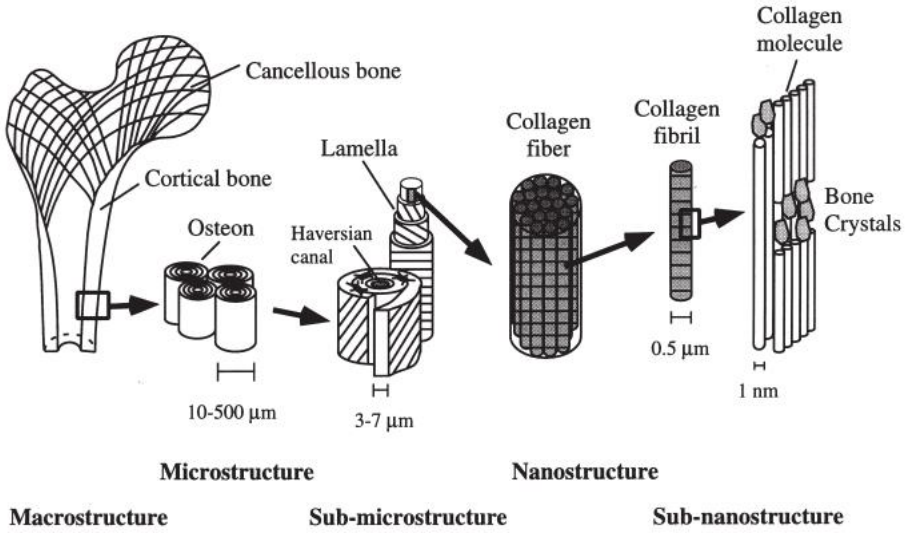

Figure 2.1 : Hierarchical structural organisation of human bone (Rho et al. 1998).

Human bone matrix consists of approximately 60% of inorganic and 30% of organic components and 10% of water phases on a weight basis. Inorganic part is composed of calcium phosphate which mostly referred as hydroxyapatite (HA) ($Ca_{10}(PO_4)_6(OH)_2$). Additionally, there are many trace elements such as copper, iodine, zinc, selenium, fluoride, manganese, which have positive effect on bone health (Zofkova, Nemcikova, & Matucha 2013). Also, the organic part is consists mainly of

collagen-I (90 wt%) in addition to other collagen types (III and VI) and various non-collagenous proteins. Bone tissue is formed its hierarchical structure from collagen fibrils (nanoscale) to lamellae (microscale) as shown in the **Figure 2.1** (Keaveny, Morgan, & Yeh 2004).

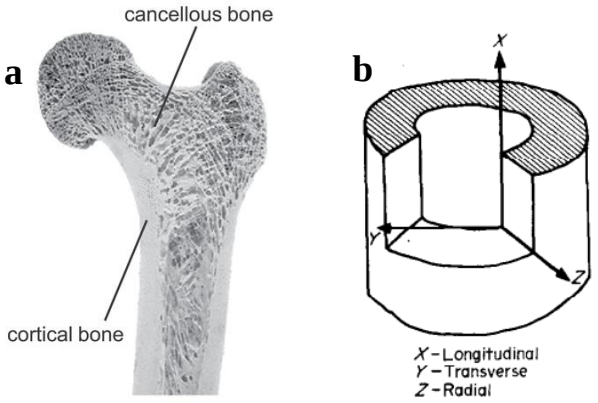

Figure 2.2 : a. Structure of bone at macro scale, b. Coordinate system for cortical bone specimen.

At macro scale, there are two types of bone; trabecular (cancellous, spongy) and cortical which are distinguished by their density and porosity. While lamellar and Haversian are tightly packed in cortical bone, cancellous bone has highly porous structure (Figure 2.2a) (Rho et al. 1998).

Mechanical properties of human femoral cortical bone was shown in the Table 2.1. Since bone has anisotropic character which means property of being directionally dependent (Figure 2.2b), tension, compression and elastic modulus values are different for longitudinal and transverse lines.

Table 2.1 : Anisotropic and Asymmetrical Ultimate Stresses and Elastic Properties of Human Femoral Cortical Bone (Reilly & Burstein 1975).

	Longitudinal (MPa)	**Transverse (MPa)**
Tension	135±15.60	53±10.70
Compression	205±17.30	131±20.70
Elastic Modulus	17900± 3900	10100±2400
Shear Stress (MPa)	65±4.00	

2.1.2. Bone remodelling

Bone is an active and dynamic tissue which has a high regenerative capacity and bone is remodelling continuously throughout life. There are three main types of cells which are responsible for this self-repairing process: osteoblasts, osteocytes, and osteoclasts (Florencio-Silva, Sasso, Sasso-Cerri, Simoes, & Cerri 2015; Kearns & Kallmes 2008) (Figure 2.3).

Osteoblasts (OBs):

OBs arise from mesenchymal cells which then differentiate into osteoprogenitor cells. These cells have a central nucleus and they produce organic bone matrix and help mineralisation to form new bone called "osteoid". Moreover, they secrete factors that activate osteoclasts. OBs found on the surface of the new bone.

Osteocytes:

Osteocytes are mature bone cells and derived from osteoblasts. Approximately 90% of mature skeleton cells are osteocytes which entrapped in matrix and responsible from bone formation. Furthermore, regulation of calcium phosphorus concentration is balanced by osteocytes.

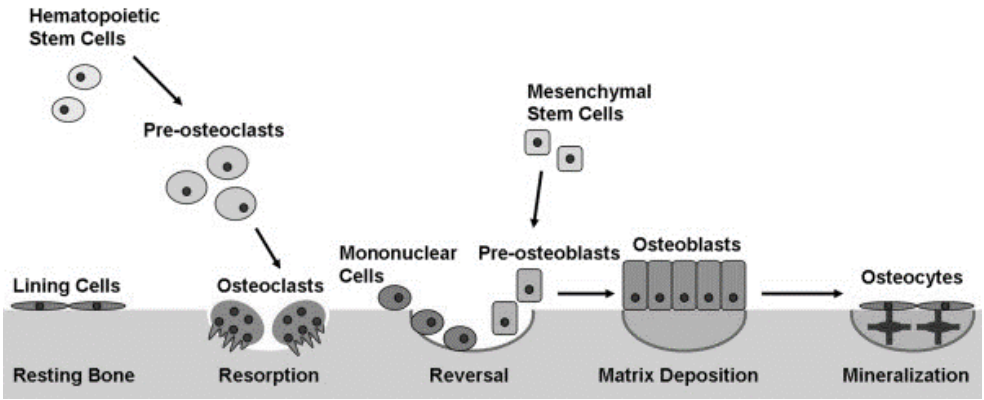

Figure 2.3 : Bone remodelling process (Kapinas & Delany 2011).

Osteoclasts (OCs):

OCs are large, poly-nucleated cells and arise from the monocyte/macrophage lineage. They are located on bone surfaces of the old, injured bone. Bone is resorbed

by osteoclast in bone remodelling. Additionally, they are exocrine cells that secrete enzymes, resorb extracellular matrix (ECM) proteins and dissolve bone minerals. At the end of the resorption, OCs undergo apoptosis which is programmed cell death.

2.2. Bone Tissue Engineering

Many different bone diseases such as bone infections, fractures and osteoporosis are more frequently seen due to the rise in the average age of population or traumatic reasons (Bose et al. 2012; Rauh et al. 2011). Since bone cannot manage to heal itself when a defect exceeds the critical size, autographs or allographs are used for bone reconstruction in order to improve bone healing (Brydone et al. 2010; Lichte et al. 2011). Although four million bone grafting are performed in the world annually, autographs and allographs have significant limitations and risks such as donor site morbidity, high infection risk and immune response (Brydone et al. 2010; Inzana et al. 2014).

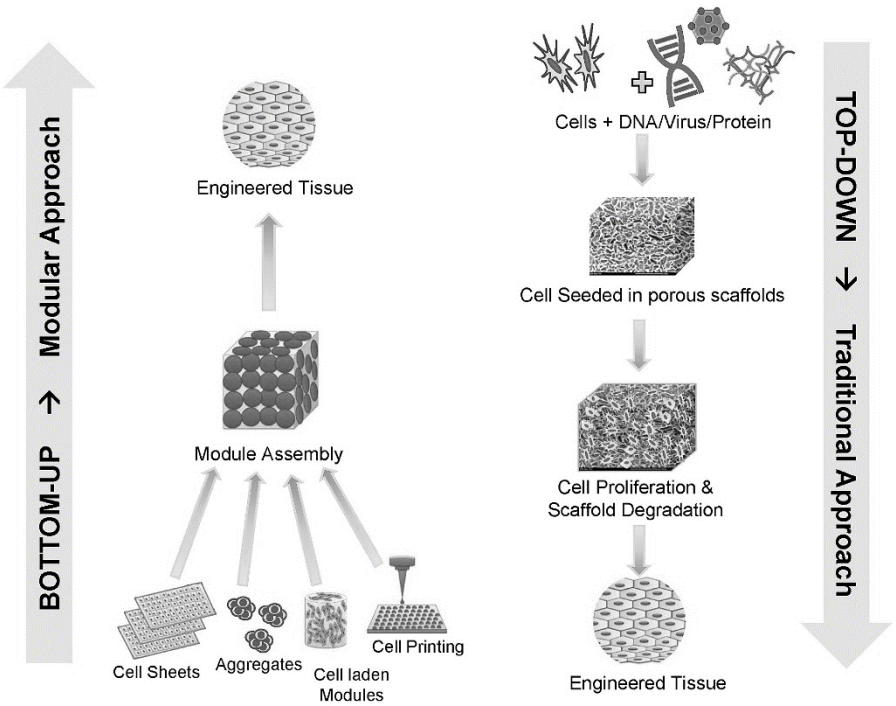

Figure 2.4 : Bottom-up and top-down approaches of tissue engineering (Tiruvannamalai-Annamalai, Armant, & Matthew 2014).

Tissue engineering (TE) offers various strategies with biocompatible and well-designed 3D bone scaffolds to lead tissue formation (Subia 2010). TE avoids

immunological responses and viral infections by using autologous cells (Stock & Vacanti 2001). There are mainly two approaches in tissue engineering; bottom-up and top-down. While in the first approach assembles the modules to reach the engineered tissue, second approach uses scaffolds for the same purpose (Figure 2.4).

Top-down tissue engineering utilizes three main tools to restore, maintain, or improve function of tissue or whole organ. These tools are cells, scaffolds and stimulus (bioactive agents or mechanical stimuli) (Subia 2010).

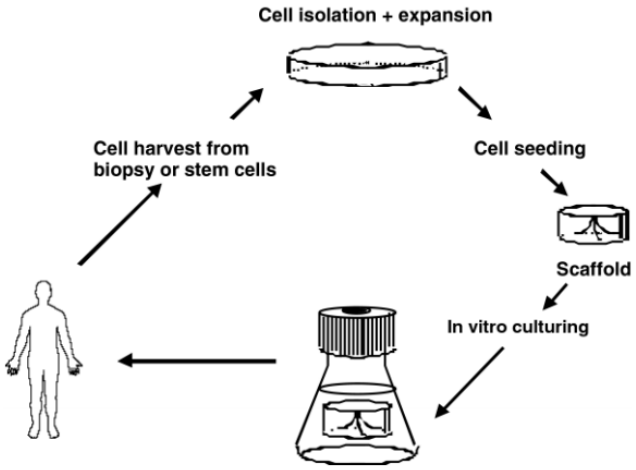

Figure 2.5 : Concepts of tissue engineering (Stock & Vacanti 2001).

As a basic concept of tissue engineering, cells are harvested from related organ (or stem cells can be collected from various stem cell sources). Then, desired cell line is isolated and cultured to increase cell number *in vitro*. Meanwhile, scaffold which should provide convenient biological and mechanical profile with natural tissue, is manufactured in 3D. Following that, cells seeded on scaffolds are cultured in a bioreactor to proliferate inside the pores of scaffolds and improve mechanical property. Afterwards, created tissue is implanted to damaged side of human body.

For deep understanding, in the following section, potential scaffold materials, zinc as a dopant of scaffolds, conventional and additive manufacturing based scaffold production techniques and stem cells will be presented and personalized tissue engineering will be discussed at the end of the section.

2.1.1. Scaffold materials

Scaffolds are not used to replace the bone tissue permanently, they leads to simulate bone growth and remodelling. Design criteria for an ideal bone scaffold were summarized by Li et al. as shown in the Table 2.2. These three-dimensional platforms should not secrete any toxic product during degradation process during bone regeneration. Also, they should be biocompatible, osteoconductive (promote cell adhesion, proliferation and form ECM) and osteoinductive (induce new bone formation) which are essential properties for scaffold materials (Bose et al. 2012). Furthermore, a well-designed scaffold should have a perfect match with defect side along with having similar mechanical properties with host bone. In addition, manufactured scaffold should be sterilisable with any technique for clinical usage (Lichte et al. 2011).

Table 2.2 : Scaffold design criteria for bone tissue engineering (BTE) (Y. Liu, Lim, & Teoh 2013).

Criteria	Function
Biocompatibility	Ability to perform its function in the host tissue without eliciting any immune response
Biodegradability	Tunable rate of degradation to match growth of new bone tissue as scaffold gets placed by new bone
Mechanical Properties	Sufficient mechanical strength to provide temporary support to the defect region and withstand in vivo loading forces
Microarchitecture	Interconnected scaffold structures to uniformly distribute stresses throughout scaffold
Osteoinductivity	Osteoinductive properties to recruit and differentiate osteoprogenitors to defect region
Porosity	Large surface area: volume and pore size to allow for tissue in-growth, neovascularisation, mass transport and osteogenesis
Surface properties	Appropriate chemical and topological properties for influencing cellular adhesion, proliferation and differentiation.

As such in biomaterials, scaffold are categorized in four groups; metallic scaffolds, ceramic scaffolds, polymeric scaffolds and composite scaffolds.

2.1.1.1. Metallic scaffolds

Porous metallic scaffolds are mostly made of titanium (Ti) and stainless steel (SS) which are biocompatible and relatively inexpensive metals. However, since metals have high compression strength and elastic modulus, it could cause stress shielding which limits mechanical stimulation and osteoblastic differentiation during bone healing. Moreover, metals are not biodegradable and may release metal ions. Due to mentioned disadvantages of metals, they are used in limited cases such as spine surgery. At the same time, various surface modifications or coatings are applied to increase bioactivity (Bose et al. 2012; Lichte et al. 2011).

Recently, magnesium alloys are developed as a biodegradable and biocompatible metallic scaffolds. Liu at al. investigated the biodegradation and osteogenic properties of magnesium scaffolds *in vivo* and they reported that it is a promising material for orthopaedics (Y. J. Liu, Yang, Tan, Li, & Zhang 2014).

2.1.1.2. Ceramics

Ceramics are commonly used in BTE because of their agreeable biocompatibility and good implant-host tissue integration. At the same time, since the dry inorganic part of bone is composed of 90 wt% calcium phosphate, ceramics are promising candidates to be used as scaffold materials to perfectly mimic the natural bone (Bose et al. 2012; Lichte et al. 2011). There are three main parameters for ceramic based materials; being bioinert, bioactive and bioresorbable which all have some benefits and limitations as shown in the Table 2.3.

Table 2.3 : Advantages and limitations of bioinert, bioactive and bioresorbable ceramics (Ducheyne 1999).

Category	Advantages	Limitations
Bioinert	Minimal biological response, High wear resistance	Limited mechanical properties in tension
Bioactive	Enhanced bone tissue response, Bone bonding	Limited tensile strength and fracture toughness
Bioresorbable	Material is replaced by normal tissue, thereby excluding possible long term effects	Rate of strength reduction may be too rapid

As it can be clearly seen from the table, the most important disadvantage of ceramic scaffolds for clinical usage potential is their low mechanical strength. Although ceramics have high brittleness, they have low wear rate. Because of their tribological characteristics, ceramics are mostly used in articulating surfaces. Another disadvantage of ceramics is that they are soluble at biological conditions easily (Y. Liu et al. 2013).

Mostly preferred ceramic based materials for BTE are calcium phosphates (CaP), bioglass and calcium sulphates (Paul & Sharma 2007). Tricalcium phosphate (TCP) and HA are classified under the group of CaP and both are highly biocompatible. CaPs were used in orthopaedic and dentistry since 1980s (Giannoudis, Dinopoulos, & Tsiridis 2005). They are available in powder, injectable, and semi-solid form to be used as bone filler. In 1969, Hench was observed that bone can bond to certain glass composition which called as bioactive glasses (Hench 1999) which have been used in various applications such as bone regeneration and implant coating (Yan et al. 2006). Finally, calcium sulfate ($CaSO_4$) is an inorganic compound which exists in three levels of hydration; anhydrous state (CaSO4, anhydrite), dihydrate ($CaSO_4(H_2O)_2$, gypsum) and hemihydrate ($CaSO_4(H_2O)_2$, plaster of Paris, bassanite).

Calcium sulfate hemihydrate is produced by heating of gypsum and removal of three quarters of its water (Coetzee 1980).

$$CaSO_4 . 2H_2O \xrightarrow{Heat} CaSO_4 . {}^1\!/_2\ H_2O + {}^3\!/_2\ H_2O \qquad \textbf{(1)}$$

Then, approximately above 200 °C, hemihydrate transform into anhydrite form;

$$CaSO_4 . {}^1\!/_2 H_2O \xrightarrow{Heat} CaSO_4 + {}^1\!/_2\ H_2O \qquad \textbf{(2)}$$

The first reported usage of Paris plaster as a bone filler in patients was in 1892 by Dreesmann (Peltier 1959). Since calcium sulfate ($CaSO_4$) is a glut in the market and has a low cost, it has been widely used biomaterials in bone regeneration more than 100 years (Beuerlein & Mckee 2010). In addition to its availability, $CaSO_4$ has various advantages such as bioresorbablity, biodegradability, good osteoconductivity and biocompatibility to be used as a bone grafting material (Asadi-Eydivand, Solati-Hashjin, Farzad, & Abu Osman 2016; Orsini et al. 2001; Pietrzak & Ronk 2000; Thomas et al. 2005; Wu et al. 2012). Moreover, it releases calcium ions which may

provide an advantage for osteoblast formation (Thomas et al. 2005). Calcium sulphate hemihydrate ($CaSO_4 . 0.5H_2O$) was studied by Sidqui et al. (Sidqui, Collin, Vitte, & Forest 1995) who reported that osteoblastic cells attach on calcium sulphate hemihydrate and osteoclasts resorb the material. Wu H. D. and his colleagues demonstrated that combination of amorphous calcium phosphate and calcium sulphate improves osteoconductivity of materials and degradation period of this composite matching with natural bone regeneration rate (Wu et al. 2012).

$CaSO_4$ was one of the earliest material used in 3D printers because of the fast setting characteristic of it (Asadi-Eydivand et al. 2016). Although this inexpensive medical grade resorbable CS has a long history in orthopaedics, powder based 3Dprinting technique may bring innovation to its usage in tissue engineering field (al Ruhaimi 2001). In contrast to its various advantages, one of the major challenge in usage of $CaSO_4$ as a scaffold material is its low mechanical resistance and high solubility as such in other ceramics.

2.1.1.3. Polymers

Polymers could be categorized as natural and synthetic. Most common natural polymers used in TE are collagen, chitosan, hyaluronic acid, and alginate. Although they are biocompatible, control on degradation rate is difficult for this group.

On the other hand, main advantage of synthetic polymers is controlled degradation rate. However, since their degradation products creates local acidic environment it could cause negative tissue responses. Poly-lactic acid, poly-glycolic acid, and poly (lactic-co-glycolic) acid are U. S. Food and Drug Administration (FDA) approved polymers. In spite of their various mechanical and biological characteristics, both natural and synthetic polymers have good processability (Bose et al. 2012).

2.1.1.4. Composites

Since, composites are combination of two or more materials, it is possible to combine advantages of two distinct materials. Bone tissue is consist of both organic and inorganic compound with completely distinct properties. Thus, polymer and ceramic combination as a bone scaffold could meet mechanical and psychological

requirements of host tissue (Bose et al. 2012). The most commonly researched polymer/ceramic composite is polyesters with CaPs (Lichte et al. 2011).

2.1.2. Simulated body fluid

Simulated body fluid (SBF) is a solution which have nearly the same ionic concentration and pH value with inorganic content of human blood plasma. When ceramic samples are soaked in SBF solutions, it is seen that their surfaces coated with calcium phosphate. SBF is used to mimic physiological body condition and biological mineralization (Bayraktar 1999). In the Table 2.4 ion concentrations of human plasma and Tas's SBF formulation were compared.

Table 2.4 : Ion concentrations of human plasma and SBF formulation of Tas (Bayraktar 1999).

Ion	Human Blood Plasma (mM)	Tas SBF (mM)
Na+	142.0	142.0
K+	5.0	5.0
Mg2+	1.5	1.5
Ca2+	2.5	2.5
HPO42-	1.0	1.0
HCO3-	27.0	27.0
Cl-	103.0	125.0
SO42-	0.5	0.5
Buffering agent	-	Tris

Biomaterials are soaked in SBF to investigate the potential apatite formation in body. When apatite layer is formed on the surface, bone forming cell will proliferate on it and fibrous tissue proliferation which occurs around foreign material will not be observed (Hench 1999).

2.1.3. Zinc oxide

Human body contains average 2-3 grams of zinc (Zofkova et al. 2013). And also, 0.0126 to 0.0217 % of human bone is zinc and this amount is higher than average of other fat-free tissues (0.0030 %) (Ito 2002).

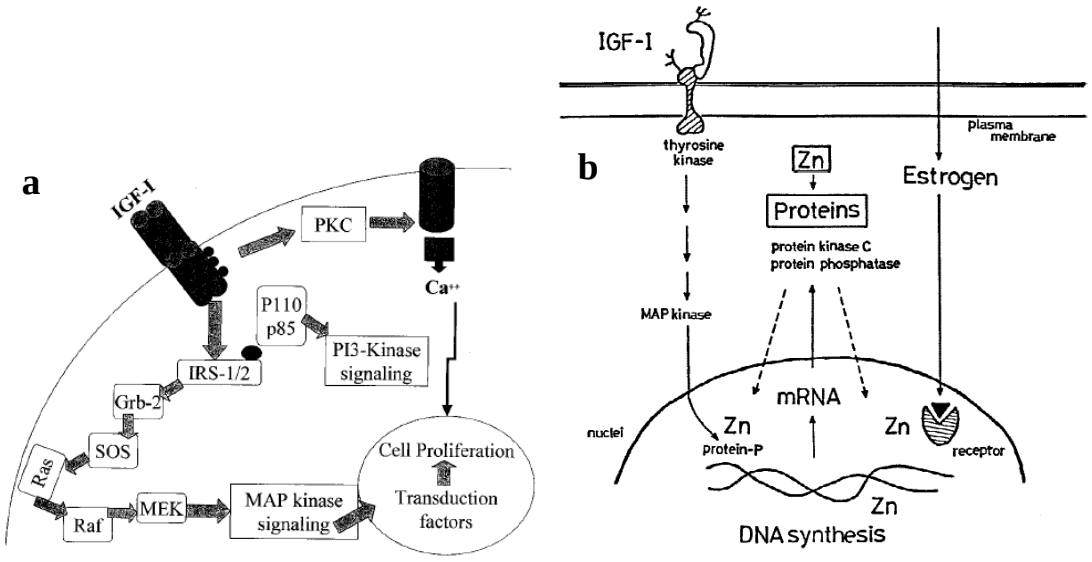

Figure 2.6 : Effect of a. IGF-I on cell proliferation pathway (MacDonald 2000), b. Zinc on IGF-I pathway (Yamaguchi 1998).

Zinc is one of the most important trace elements in human body and known to aid cell proliferation, differentiation, regulation of DNA synthesis, enzymatic functions and also has an positive effect on bone formation (Alhava et al. 1977; MacDonald 2000; Paul & Sharma 2007). Growth and differentiation pathways of cells are composed of complex cascades which various molecules such as hormones and transcription factors have special roles. And zinc is one of the essential elements which is involved in cascades of many signalling pathways in eukaryotes (Beyersmann & Haase 2001).

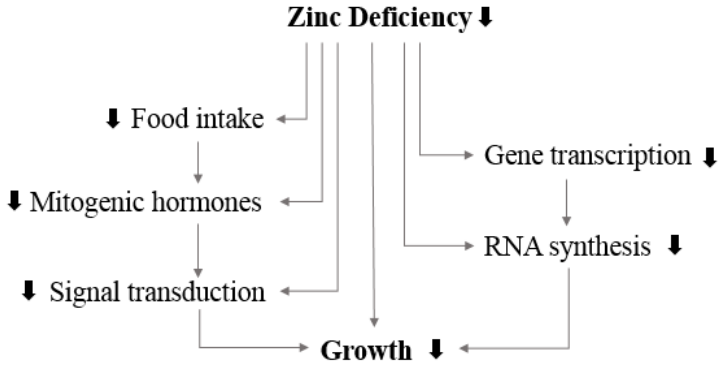

Figure 2.7 : Effects of zinc deficiency (MacDonald 2000).

Growth inhibition and decreased food intake are major symptoms of zinc deficiency (Figure 2.7). Growth is regulated by hormones such as growth hormone (GH) and

insulin-like growth factor-I (IGF-I) (Figure 2.6(a)), although hormonal changes are not fully lightened, it is know that they are affected by zinc deficiency shown in the Figure 2.6(b) (MacDonald 2000).

By the help of deep literature research, it would be clearly seen that many researches have combined the advantages of zinc and ceramic to mimic the natural bone better. Ito et al. observed growth rate of MC3T3-E1 cells on 0.6 to 1.26% zinc containing ZnTCP/HA ceramic and conclude that addition of ZnO significantly increased cell proliferation and alkaline phosphatase activity. On the other hand, zinc content higher than 1.26% caused toxicity on cells (Ito 2002). Kewamura et al. used 0, 0.063, 0.316 and 0.633 wt% ZnO included ZnTCP/HA and they report that bone formation increases 51% in 0.316 % ZnO group compared to control (Kawamura et al. 2000). Bandyopadhyay et al. studied on 0.25, 0.5 and 1 % ZnO addition to TCP. Although they observe the highest density in 1% added group, since some concerns about cytotoxicity of ZnO higher than 0.33%, they continued to their further experiments with a group of 0.25% (Bandyopadhyay 2006). Calcium sulfate hemihydrate scaffolds with zinc concentrations of 0.074, 1.97, 3.05 and 4.21 wt% were investigated in terms of cell viability and activity by Hesaraki et al. While the maximum alkaline phosphatase (ALP) activity was achieved in a content of 0.74 wt% Zn group, they reported that higher concentrations more than 1.97 wt% causes toxic behaviour on G929 cells (Hesaraki, Nemati, & Nazarian 2009)

2.1.4. Scaffold manufacturing techniques

2.1.4.1. Conventional techniques for scaffold fabrication

Solvent casting

Solvent casting method is based on dissolution of polymer in organic solvent, casting polymeric solution into the mould and providing sufficient time for evaporation of solvent. Following, polymeric layer which adhere to mould could be created. Also, it could be combined with particulate leaching (Subia 2010).

Gas foaming

In this techniques, polymer exposure to high pressure CO_2 (800 psi) to create highly porous scaffold. Pore intensity could be increased by using higher amount of CO_2 gas. In the same manner, adding porogens such as salt, sugar and wax into polymer increases porosity (Subia 2010).

Electrospinning

Electrospinning is used to create polymeric fibres from nano to macro scales. In this technology, electrical field is generated by high voltage between the nozzle and ground. Polymer is pumped by using a syringe in the electrical field and polymer jet is accumulated on a ground or on a rotating collector. Fine, special oriented fibres could be created by this versatile technique (Figure 2.8) (Greiner & Wendorff 2007).

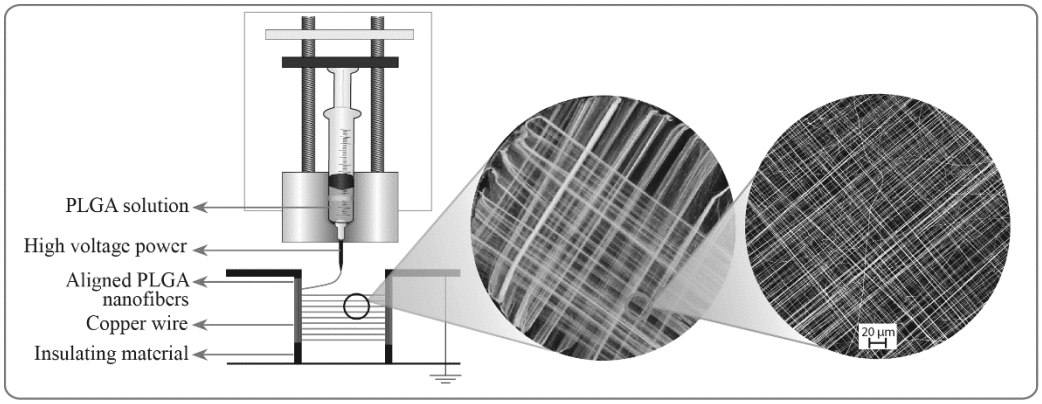

Figure 2.8 : Electrospinning setup.

Particulate leaching (porogen, salt leaching)

In this method, porogens such as salt, sugar and wax mixed with a scaffold material. At the end of the solidification process of mixture porogens will act as pore holder. Particulate leaching is one of the best techniques to have a control on size and density of pores.

Freeze drying

In freeze drying technique, firstly, polymer is dissolved in a solvent. Then, the solution is frozen to remove the solvent which is performed using by lyophilisation

under high vacuum to create porous scaffolds. Pore sizes controlled by freezing rate (Subia 2010).

Self-assembly

In self-assembly, molecules are organized spontaneously. One of the most common self-assembly methods is amphiphilic peptide sequence. In this technique, hydrophobic and hydrophilic peptides interact with each other in aqueous solution by using non-covalent bonds and create fast recovering hydrogel. Much thinner fibres could be produced by using self-assembly than other techniques (Subia 2010).

Table 2.5 : Advantages and disadvantages of conventional scaffold manufacturing techniques (Serra 2014; Subia 2010).

Method	Advantages	Disadvantages
Solvent Casting	▪ Simplicity ▪ Low cost	▪ Retention of toxic solvent ▪ Shape limitations ▪ Low interconnectivity
Gas Foaming	▪ Organic solvent ▪ High temperature are not required	▪ Low pore and geometry control
Electrospinning	▪ Structural features similar to extracellular matrix, high aspect ratio and surface area	▪ Organic solvent are used ▪ Low pore and geometry control
Particulate Leaching	▪ Control over pore size and density	▪ Inadequate pore interconnectivity
Freeze drying	▪ No need to separate leaching	▪ Small pore size ▪ Long process time
Self-assembly	▪ Control over porosity and fibre diameter	▪ Expensive material ▪ Complex design parameters

2.1.4.2. Additive manufacturing

Additive manufacturing (AM), has been introduced since late 1980s (Khoo 2015). Unlike conventional production techniques additive manufacturing builds up the final geometry layer by layer. It also called as (solid) free form fabrication (SFF, FFF) or rapid prototyping (RP) (Upcraft 2003).

AM techniques has various advantages in comparison with conventional scaffold production techniques such as; excellent control over geometry, controllable and interconnected porosity, production of variable designs at the same time, material variety, minimum waste, fast and automatized manufacturing.

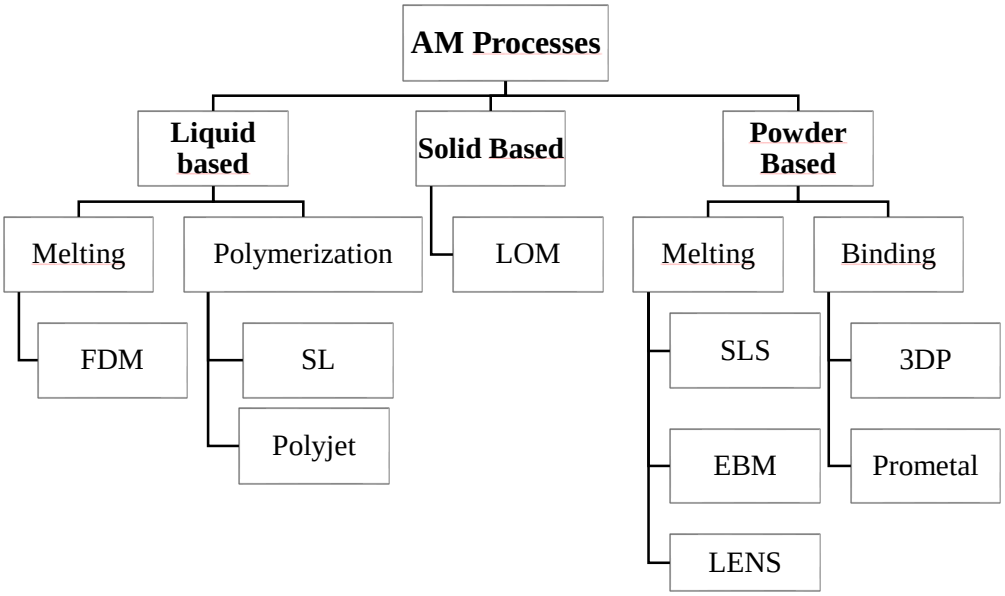

Figure 2.9: AM Categorization according to raw material phase (Wong & Hernandez 2012) .

AM processes could be categorized into three main groups as liquid, solid, and powder based in terms of material phase. Stereolithography, selective laser sintering, laminated object manufacturing, fused deposition modelling and 3D printing will be explained in this section.

Stereolithography

Stereolithography (SL, SLA) was developed by 3D Systems Inc in 1988 (Gibson 2015). This technique uses UV light to solidify the photo-sensible liquid polymer in specific locations of each layer till the 3D models created (Hutmacher, Sittinger, & Risbud 2004; Wong & Hernandez 2012). In addition, higher resolution micro-

stereolithography which has layer thickness at least 10 µm is also available (Wong & Hernandez 2012). Furthermore, the residual polymer can be reused.

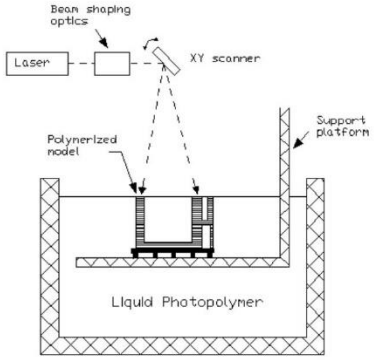

Figure 2.10 : Working principle of stereolithography (Krar 2003).

Selective laser sintering (Direct metal sintering)

Selective Laser Sintering (SLS) was patented by DTM in 1986 (Gibson 2015). This is a powder based fabrication technology that uses CO_2 laser to fuse layers of plastic, metal, ceramic and composite powders. The chamber is heated until the melting point of the material in specific locations. Moreover, residual powder can be reused (Hutmacher et al. 2004; Wong & Hernandez 2012).

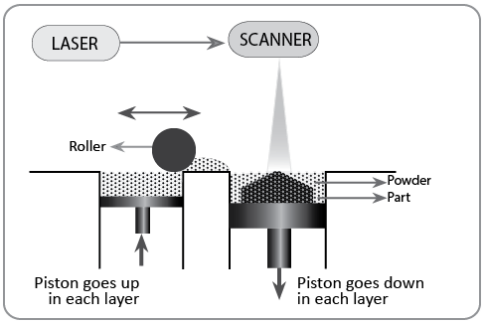

Figure 2.11 : Working principle of selective laser sintering.

Laminated object manufacturing

Laminated Object Manufacturing (LOM) was patented by Helisys in 1986 (Gibson 2015). In this technique paper, plastic or polymer sheet form materials are sliced layer by layer with carbon dioxide laser and then layers are laminated by pressure or heat to form 3D model (Hutmacher et al. 2004; Krar 2003; Wong & Hernandez 2012). However, its major disadvantage is that residual sheets cannot be reused.

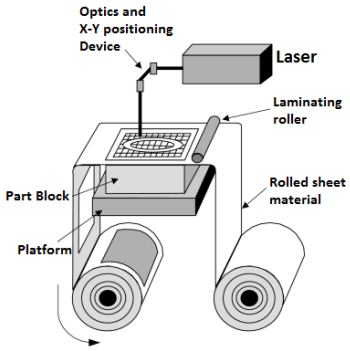

Figure 2.12 : Working Principle of Laminated Object Manufacturing (Upcraft 2003).

Fused deposition modelling

Fused Deposition Modelling (FDM) was patented by Scott Crump from Stratasys Company in 1989 (Gibson 2015). In this technology material filament are melted and deposited (Upcraft 2003). FDM is one of the most preferred AM technique because of its cost efficiency and high quality.

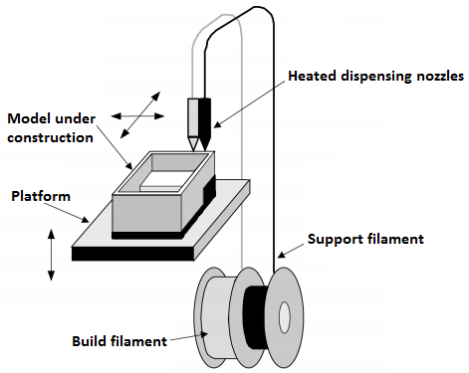

Figure 2.13 : Schematic representation of FDM (Upcraft 2003).

Three dimensional printing

Three Dimensional Printing (3DP) was patented by a group from MIT in 1989 (Gibson 2015). In this manufacturing technology, the liquid binder is dispersed onto powder material to bind it together (Upcraft 2003). One thin layer of powder material is dispersed on a platform, following that the binder is sprayed onto the laid powder layer in powder based 3DP technique. The binder binds the powders to form a single 2D layer, so a sliced 2D profile of a computer model is created. This process occurs

many times to fabricate a 3D structure layer by layer until the whole model is completed (Lichte et al. 2011).

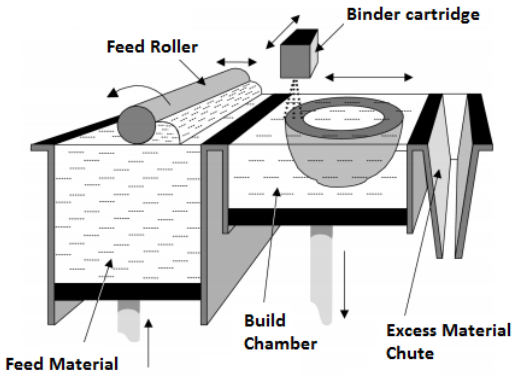

Figure 2.14 : Schematic view of 3DP process (Upcraft 2003).

Each technique have both advantages and disadvantages as shown in the Table 2.6. Convenient method is chosen according to raw material and desired properties.

Table 2.6 : Comparison of 3D Scaffolding methods (Butscher 2013).

Technique	Advantages	Disadvantages
SLA	▪ High accuracy	▪ Limited choice of materials ▪ (Photopolymer needed) ▪ Support structure needed
SLS	▪ High mechanical properties ▪ No support structure needed	▪ High processing temperature ▪ Powder can be trapped inside the body
LOM	▪ Low cost	▪ Waste material
FDM	▪ no require for chemical post-processing ▪ no resins to cure ▪ less expensive ▪ high quality	▪ High temperature ▪ Thermoplast polymers required ▪ Mechanical anisotropy ▪ High temperatures
3DP	▪ Versatile ▪ High porosity can be achieved ▪ Broad material range ▪ No support structure needed ▪ Cost efficient	▪ Small green strength ▪ Depowdering difficult due to weak bonding between particles ▪ Powder can be trapped inside the body

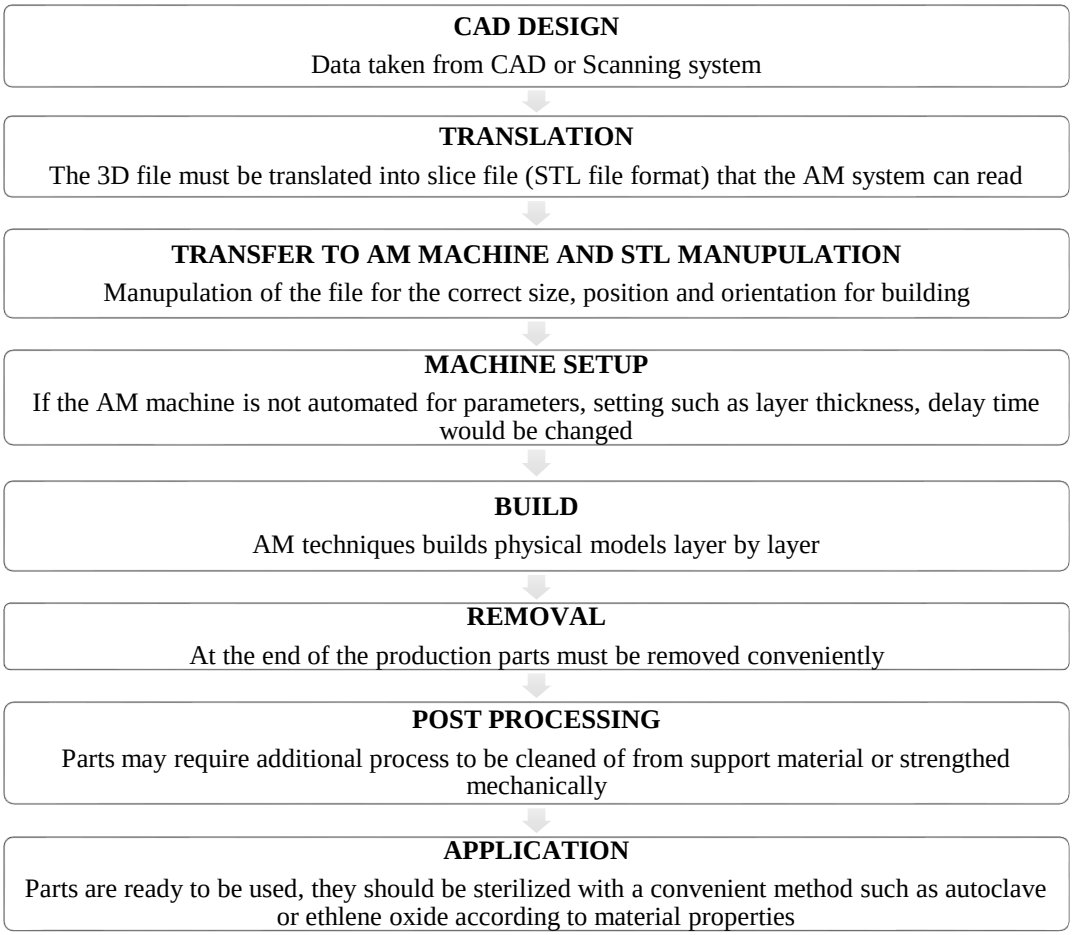

Figure 2.15 : Additive Manufacturing flow chart (Gibson 2015; Krar 2003).

Post Processes

At the end of the manufacturing, it is possible to apply some post processes to increase quality of fabricated scaffolds. Although it is time-consuming process, it enhance mechanical and physical quality of the materials. Post-printing manipulation, depowdering, coating, sintering and infiltration are some of those post process applications. Depowdering is removal of loose powder with brushing, blowing air, vacuuming, vibration, and wet depowdering (ultrasonicating, microwave-induced boiling and CO_2 bubble generation in soda water). Coating is usually done with polymer-particle paste or slip casting to improve surface. Sintering and infiltration are applied to increase strength of structures, but scaffold structure is exposed to temperature that may causes shrinking in sintering. Dipping part,

aerosolizing infiltrant and spraying the part are infiltration techniques to get high density structures without the large shrinkage (Utela et al. 2008).

2.1.5. 3D cell and organ printing

3D printing applications would be categorized into two groups in TE. First one is indirect printing which 3D printed scaffolds are produced by additive manufacturing technique. Following that cells are inoculated on scaffolds by using conventional TE applications. This technique covers top-down tissue engineering. Contrary to this, the second technique, bottom-up tissue engineering application, is direct cell printing which provide delivery of scaffold material, living cells, and stimuluses all together (Sun, Darling, Starly, & Nam 2004).

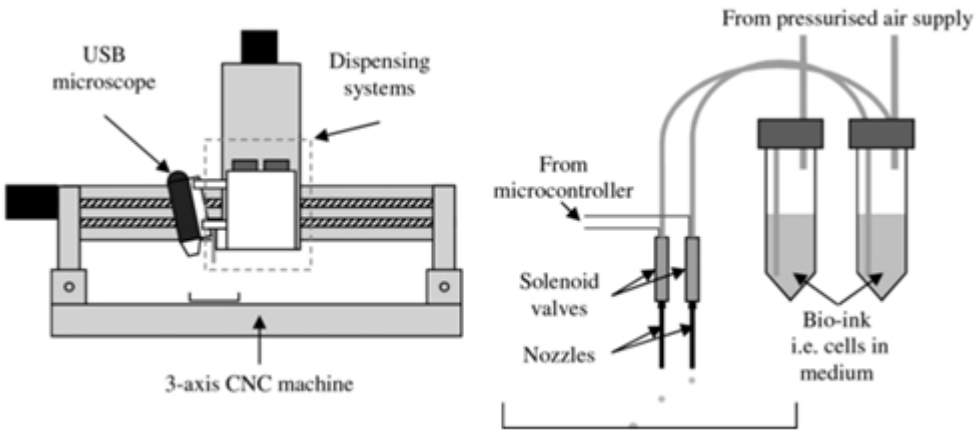

Figure 2.16 : 3D cell printing set-up (Faulkner-Jones et al. 2013).

Organ and tissue printing become popular in 2000s (Xu 2014). This technique enables to place cells more quickly and accurately. 3D cell printer can be designed with multi-nozzles which will distribute different cell types (Figure 2.16). In this way, it is a promising technique to design vessel network which is the main drawback of TE (Varghese et al. 2005). Cells are suspended in bio-ink solution which includes medium, polymer solution such as collagen and growth factors. Although there are commercial bio-printers on the market this system could be modified from ink-jet printers by displaying paper-feed mechanism and adding step motor control for movement in third axis (z-axis).

While basic models are created easily for cell and organ printing, since living tissues are composed of multiple cell types and vascular network in complex design, for 3D

tissue and organ printing, a model of detailed anatomy and morphology which called as bio-blueprint is required (Xu 2014). During printing process cells are deposited to right places in accord with this description. Bio-blueprint model includes; description of inner and outer architecture of an organ heterogenic tissue based and individual tissue boundaries, description of vascular network of the organ and a database about geometry, heterogeneity and vascularity (Sun et al. 2004).

2.1.6. Personalized bone substitutes

With emerge of SFF techniques, a new field have branched from TE that of computer-aided tissue engineering (CATE). This field contains design by using CAD, and manufacturing by using SFF. CATE highly interdisciplinary area which combines information technology, material science, mechanical engineering and TE. CATE mainly have three applications (Sun et al. 2004);

1. Computer-aided tissue modelling
2. Computer-aided scaffold design and manufacturing
3. Computer-aided tissue informatics

Computer aided tissue models could be captured by using CT (computed tomography), MRI (magnetic resonance imaging) and optical microscopy and re-constructed. Although captured 3D data can be directly altered to STL (stereolithography) format which is required for additive manufacturing and printed with AM system, due to many advantages such as modification flexibility model are converted into a CAD-based solid model.

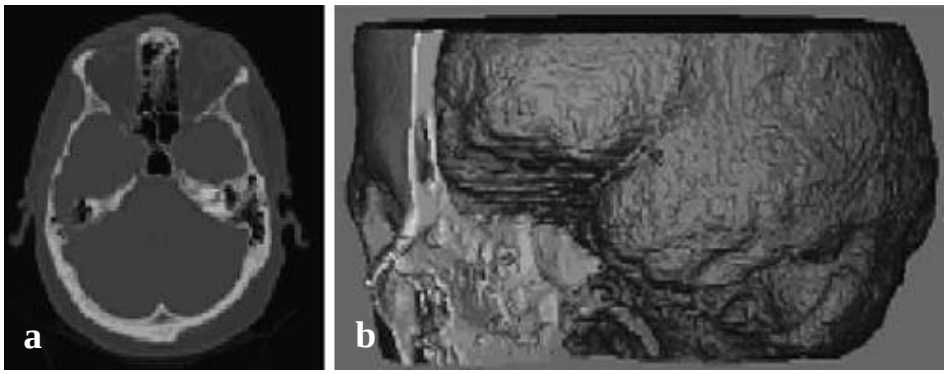

Figure 2.17 : a. 2D CT image, b. CT-derived 3D model of skull and brain (Sun et al. 2004).

CT and μ-CT(micro-CT) which used to show internal structure of sample, creates X-ray radiation and images the sample according to different absorption rates of different regions on it. Since μCT has high resolution, it is capable of showing internal structures of tissues. As a principle of CT, it created 2D (two-dimensional) images to create 3D representation. MRI can image soft tissues in addition to hard tissue. The output is 3D model created from 2D slices (Figure 2.17). Although MRI has capability to visualize various tissues, its resolution is lower than CT and optical microscopy (Xu 2014).

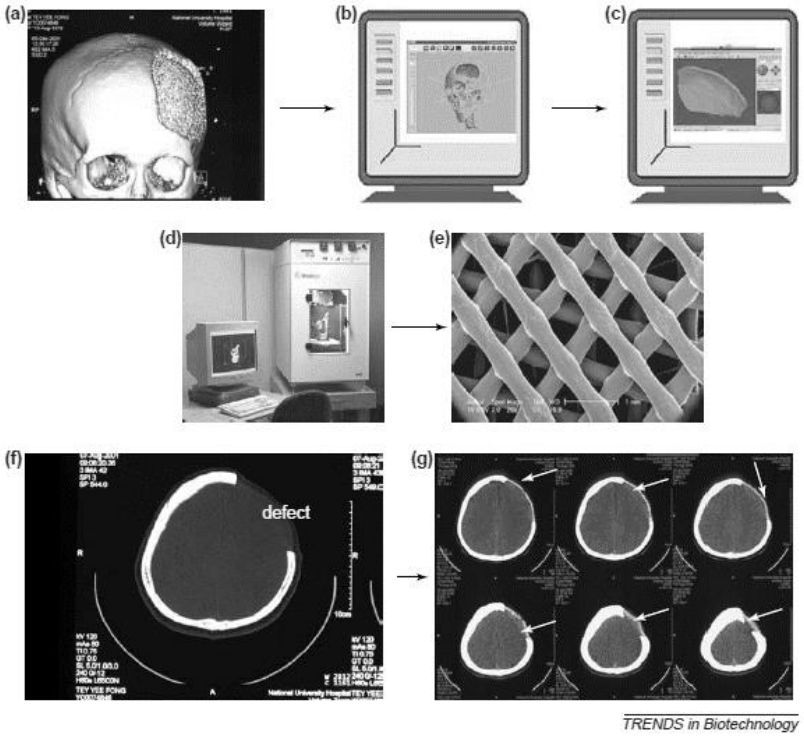

Figure 2.18 : Production of patient-specific bone grafts. a. CT scan data of patient, b. RP system software is captured to generate 3D model, c. Remodelling of defect side, d. Scaffold building, e. Scaffold design, f. defect side from sliced data, g. defect-scaffold match (Hutmacher et al. 2004).

The main aim in personalized bone substitutes is to produce defect-matching scaffolds. There are certain essential steps for production of patient specific implants or grafts (Figure 2.18). Firstly, 3D model of defect side should be captured by CT scan and imported to the program. If the defect side has a healthy mirror image on body (such as deficient right hand, health left hand), CT data of the health area is captured to be used as a scaffold model. Otherwise, this model should be created by CAD (Computer Aided Design) software such as Solidworks or Inventor. After

designing the inner architecture (flat or porous) and outer shape of the scaffold or implant, model is produced slice by slice by convenient AM technique according to material type. 3D printing is one of the best techniques particularly for custom designs on artificial bone applications because of the high controllability, design independency, fast producibility, reproducibility, no waste material, variety of material. Finally, patient specific model is sterilized and ready to be used *in vitro* or *in vivo*.

As a top-down TE approach, cells which are isolated from individual's body is inoculated on manufactured scaffold for personalized bone scaffold applications after sterilization process. Osteoblastic cell or stem cells could be used in this process.

Stem cells are unspecialized cells and capable continuous of self-renewal. They can give rise to specialized cell types (Sharma 2014). Mesenchymal stem cells (MSCs) are found in multiple tissues including bone marrow. Although 0.001%-0.01% of the entire bone morrow cells, MSCs can be expanded by using cell culture techniques. They can differentiate into osteoblasts. The main advantage of usage of MSCs in TE is that they can be used without immune rejection. Following inoculation of BMSC (bone marrow stem cell) to the scaffold, they are subjected to osteogenic differentiation by using various environmental and biological factors (Eslaminejad & Faghihi 2011).

3. MATERIAL AND METHOD

3.1. Manufacturing

3.1.1. Powder preparation

Commercial powder of 3D printer (Projet 160, 3DS USA) purchased from 3D Systems. Asadi-Eydivand et al. indicates that commercial powder (calcium sulfate hemihydrate, CSHH) of 3DS printers has a particle size distribution 10%, 50% and 90% of powder below 0.64, 27.36 and 68.83 μm, respectively (Asadi-Eydivand et al. 2016).

High purity zinc oxide (ZnO) was purchased from Merck (USA). Powder was doped with 0.1 wt%, 0.3 wt% and 0.5 wt% ZnO.

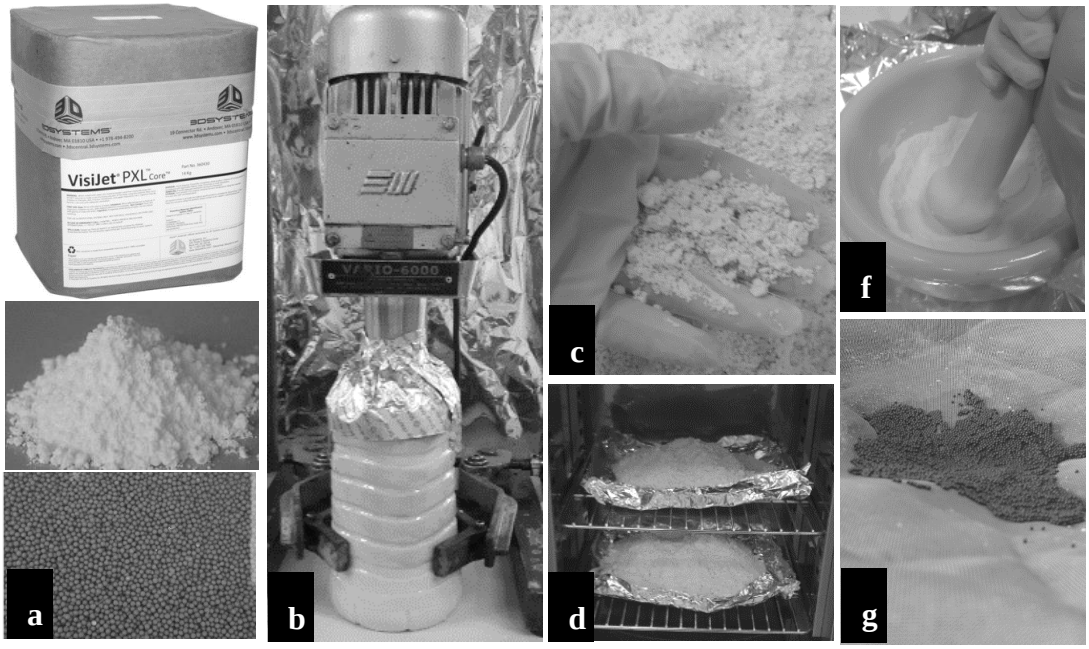

Figure 3.1 : Powder preparation process a. CSHH powder, zinc oxide and zirconia milling media (respectively), b. Homogenisation process, c. humid mixture after ventilation, d. powder mixture in drying oven, f. Pestling process, g. Sifting and removing the milling media.

0 wt %, 0.1 wt %, 0.3 wt % and 0.5 wt % zinc doped powder was prepared by following reference study (Fielding, Bandyopadhyay, & Bose 2012).

ZnO in varying concentrations (0 %, 0.1 %, 0.3 % and 0.5 %), 3 kg of powder, 1 kg of 1 mm zirconia milling media and 2 litre ethanol added for each group and mixed with mixer (Yokes Mixer Vario 6000, Turkey) for 2 hours at 250 rpm.

At the end of the 2 hours blending, mixture was spread on a tray and ventilated to evaporate ethanol without ossification at room temperature for 24 hour. Following that, the mixture transferred on aluminium foil and placed in a 60 ºC of drying oven for 48 hours. Then, the agglomerated mixture was pestle roughly and the mixture was sifted to remove the milling media with sieve. Following that, mixture was dried for another 24 hours in drying oven.

3.1.2. Scaffold design and fabrication

CAD files of test samples were created by CAD software (Autodesk Inventor Professional 2014, USA) as a requirement of 3DP process. Cylindrical block scaffolds Ø 10 mm, 5 mm height and Ø 10mm, 10 mm height was designed for cell culture and compression tests respectively. All experiments were performed by using non porous block samples to test solubility, mechanical and biological property of the material. But yet, 500 µm, 750 µm and 1000 µm porous scaffolds were designed to check the solubility and to optimize the pore size and intensity as a preliminary research for future study (Figure 3.2).

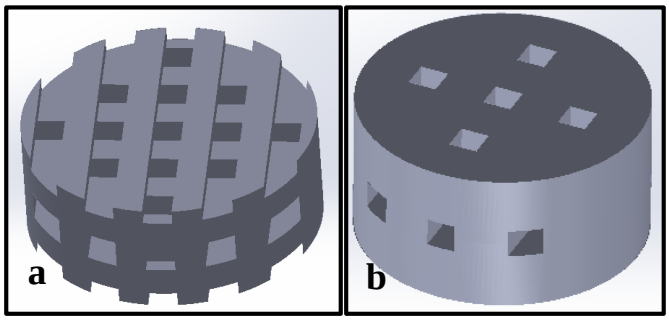

Figure 3.2 : CAD models of 3D printed porous scaffolds.

Following the design process, they were exported as .stl (surface tessellation language, stereolithography) which is the file format allowing to define 3D models using just triangle meshes. STL format can be directly imported to AM devices. Data were imported to 3D printing software (3DP Projet X60, Ver. 1.01, USA) where models were sliced by a slicing algorithms itself.

Figure 3.3 : Sample production process a. emptying and cleansing printer feeding chamber, b. printing parts with loaded powder, c. collecting samples from building area, d. depowdering loose powders by using air blowing e. pre-baked samples, f. sintered samples, g. sintered and non-sintered samples, h. all manufactured groups.

After preparation of powder mixture for each groups (4 group), powders was loaded to 3D printer starting from control and continued by increasing concentrations. The main drawback was to cleanse 3D printer at the end of the each printing process not to lose control on zinc concentrations of groups. 2D sliced layers were printed layer

by layer by the 3D printer (Projet 160, 3D Systems, USA). Printing process continued till the 3D model was physically formed. Commercial powder (3DS, Visijet, PXL, Core, Osha, USA) and water based binder (3DS, Visijet, PXL, Clear, Osha, USA) were used as consumables in 3DP process. The binder of 3D printer was Visijet PXL which is formulated as 2-pyrrolidone. It is colourless aqueous solution which has 98% water content. The pH of the binder at 20 °C is 9.8, its boiling point is 100 °C and it has a density of 1 g/cm^3 according to safety data sheet of the material. The viscosity is similar with water (Asadi-Eydivand et al. 2016).

One layer of powder thickness was 100 μm in all prints, so the resolution of printing process was also 100 μm. At the end of the printing process all scaffolds were kept in the building platform for 90 min at ambient temperature. Samples were cleaned by blowing air to get rid of loose powders after printing as a post process.

3.1.3. Sintering

After printing and blowing air processes, scaffolds were sintered for 2 hours at 1150 ˚C at furnace (Protherm Furnaces, Turkey). Since the CSHH release corrosive gas of ammonium sulphur during heating process, materials were pre-baked for 2 hours at 300 ˚C at oven (Luxell Lx 3685, Turkey) not to corrode resistances of furnace. Required temperature in order to remove the water and the ammonium sulphate was determined by Teoreanu et al. (Teoreanu, Preda, & Melinescu 2008). After that samples were ready to be fused by sintering.

Tamman temperature is the temperature which two particle start to migrate each other for sintering. So, sintering temperature should be between tamman temperature and melting temperature ($T_{melting} > T_{sintering} > T_{tamman}$) (Iribarne 1997). Since the tamman and the melting temperatures of CSHH was indicated as 416 °C and 1450 °C respectively, the final sintering temperature should be determined between these values (Marsh 1985). β-CSHH have a possibility of transforming into α-CSHH above 1200 ºC. Therefore, 1150 ºC was applied for best densification and to have best mechanical and physical properties (Figure 3.4) (Iribarne 1997).

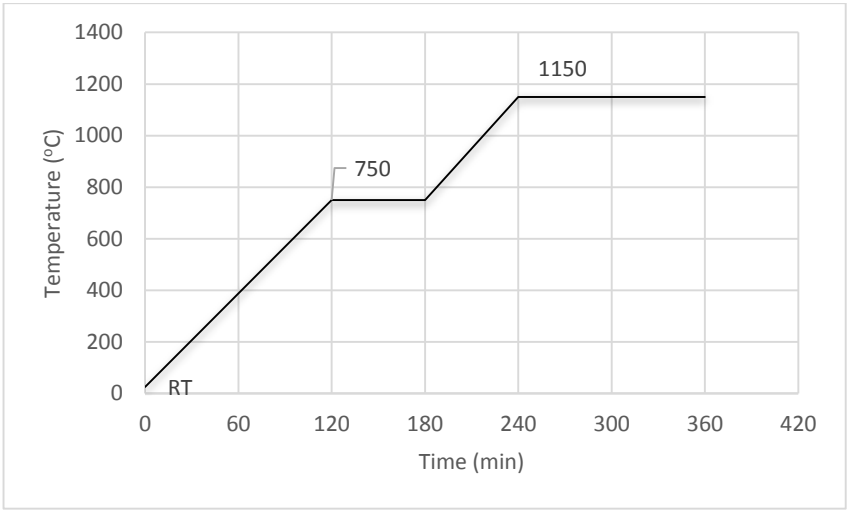

Figure 3.4 : Sintering cycle of CSHH scaffolds for all compositions.

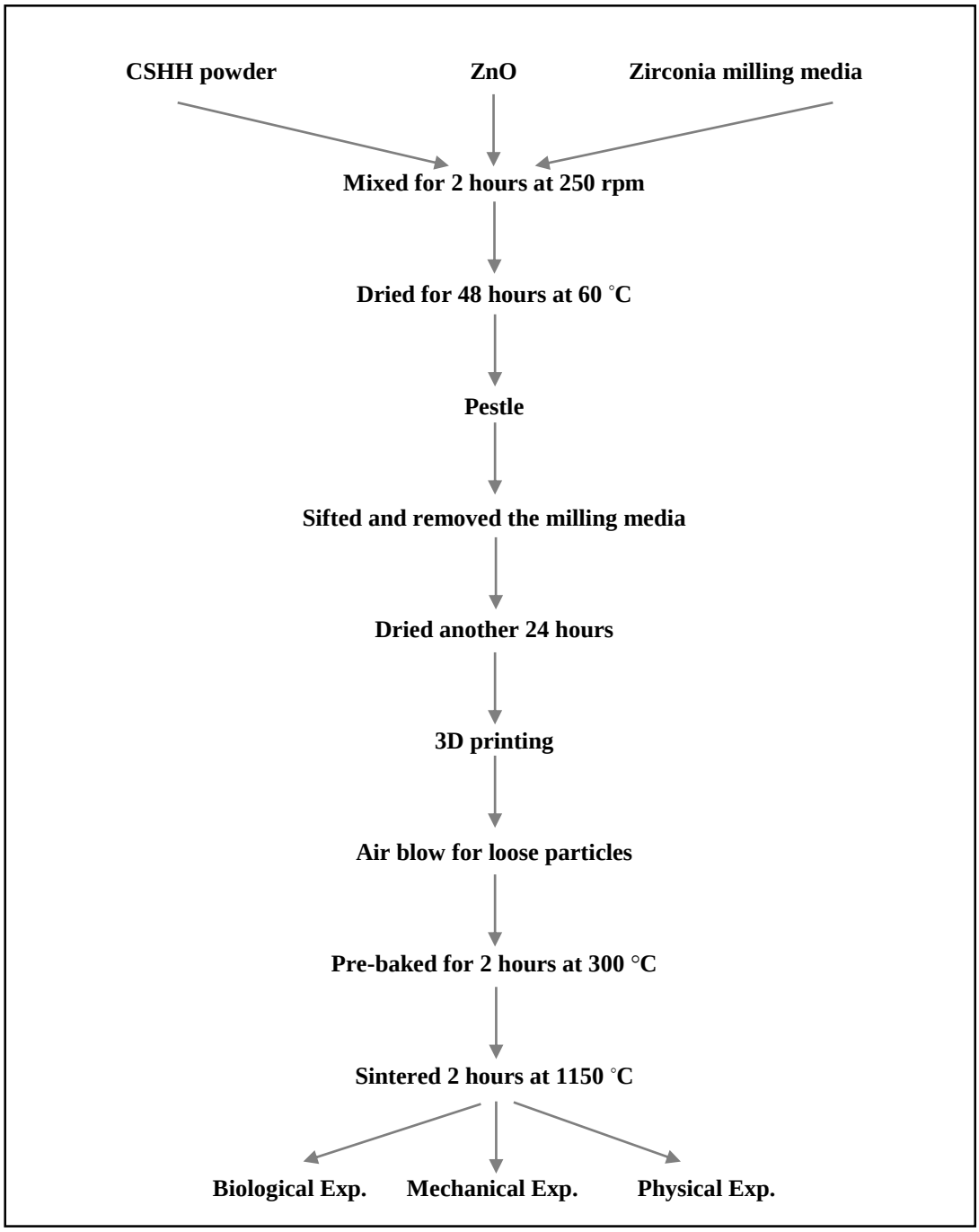

Figure 3.5 : CSHH scaffold production and characterization process flow.

3.2. Analysis

3.2.1. Wettability measurements

The wettability of CSHH samples (n=3) were measured using a contact angle meter (Biolin Scientific, Thetalite, Sweden). 4.5 µl of distilled water applied on CSHH sample's surface to measure the water contact angle under a CCD camera at ambient temperature.

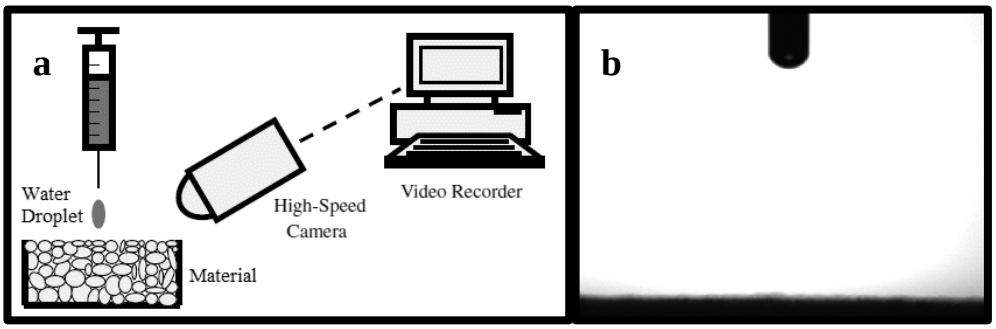

Figure 3.6 : Contact angle a. setup (Zhou, Buchanan, Mitchell, & Dunne 2014), b.view of 3D printed sample.

3.2.2. X-ray diffraction (XRD) analysis

XRD was done to observe if there were different phases of CSHH after zinc addition, printing process and also sintering compared to green, pure CSHH under the same conditions. Non-printed powders were used directly. Since powder form sample is required for XRD analysis, 3D printed green and sintered samples were pestle to have fine particles. X-ray diffraction (XRD) patterns of samples were obtained by using Philips X-Pert Pro Diffractometer using Ni-filtered Cu Kα radiation (λ= 1.54 Å) operated at 45 kV and 40 mA. The data were collected in 2θ angle ranged from 5° to 80°. The scan step size and time per step were set to 0.03°and 10 s, respectively.

3.2.3. Thermogravimetric analysis (TGA)

Thermogravimetric analyses of the samples were conducted by using STA (TA Instruments) at a heating rate of 10 °C/min under nitrogen atmosphere. The analyses were conducted in the range 30-900°C.

3.2.4. Thermomechanical analysis (TMA)

The linear thermal expansion coefficient (LCTE) was measured using TMA equipment with 0.1 μm and 0.1 mN load displacement resolution (TMA-Q400, TA Instrument).

Before the TMA the height of the test specimens was measured using a digital micrometer. The quartz probe was put into contact with the top of the test specimen. Linear thermal expansion of the test specimen was transmitted to the probe that was connected to LVDT-transducer, which allowed vertical movement of the probe to be monitored on the y-axis of the recorder. Two thermocouples were located close to the specimen and temperature variation was displayed on the x-axis of the recorder. LCTE was measured during a programmed heating rate of 10 °C/min from room temperature -30±1 to 120±1 °C. Expansion mode with a constant compression load of 0.02 N was applied to the specimen in the testing process.

3.2.5. Mechanical tests

Mechanical properties of 0; 0.1; 0.3 and 0.5 wt% ZnO containing CSHH samples (n=3) were evaluated by compression tests using a computer-controlled Shimadzu Autograph AG-IC Series universal testing machine (Shimadzu Corp., Japan) equipped with a 500N load cell. Trapezium X software was used for machine control and data acquisition.

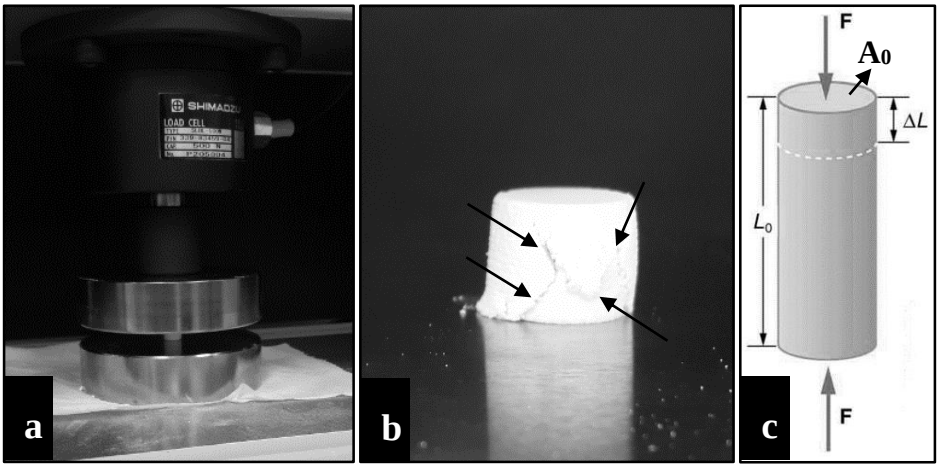

Figure 3.7 : a. Compression test set-up, b. analysed sample, c. calculation parameters.

All tests were carried out at cross-head speed of 0.33 mm/min at the room temperature. Cylindrical samples with average diameter of 10 mm and the average height of 10 mm were used.

The stress and strain were evaluated by the following formulas (Domingos et al. 2013);

$$\sigma\ (stress) = \frac{F\ (load)}{A_0\ (cross\ section)}\ , \qquad \varepsilon\ (strain) = \frac{\Delta h\ (heigh\ variation)}{h_0\ (initial\ height)}$$

3.2.6. Cell viability

3.2.6.1. Cell culture

Bone marrow stem cells (BMSCs) (Sigma Aldrich, St. Louis, USA) were used in the current study. The cells were cultured in Dulbecco's Modified Eagle's Medium (DMEM, Sigma, USA) supplemented with 10% heat-inactivated fetal bovine serum (Sigma, USA), 2 mM L-glutamine (Genaxxon Bioscience, Germany) and 0.1% penicillin/streptomycin (Genaxxon Bioscience, Germany) at 37 °C in a 5% CO_2 humidified environment. After a sub-confluent monolayer was achieved, cells were detached by gentle digestion with 0.25% trypsin/EDTA (Genaxxon Bioscience, Germany) counted with a haemocytometer, and suspended in fresh media before seeding onto scaffolds.

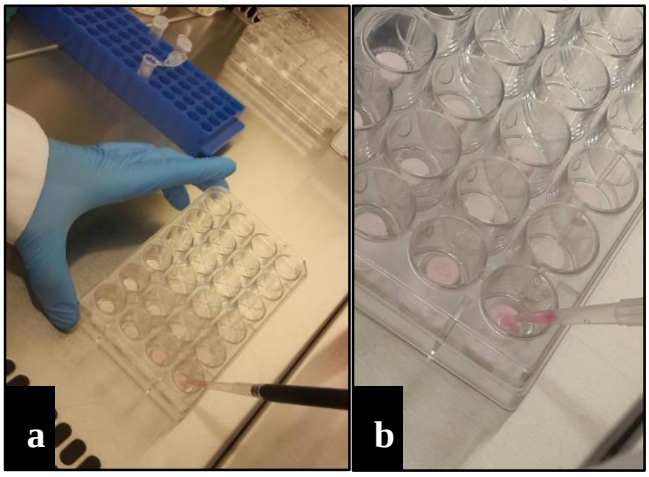

Figure 3.8 : Inoculation of cells on CSHH scaffolds.

3.2.6.2. Culture on 3D printed scaffolds

Prior to cell seeding scaffolds were autoclaved (JSR, Korea) at 121 °C for 15 minutes. Then, they were immersed in non-sterile Phosphate Buffer Saline (Genaxxon Bioscience, Germany) over night. Scaffolds have been planted in 24-well plate (Thermo Scientific, USA) were conditioned with complete culture medium for 2 hours at 37 °C. Next, cells were harvested from cell culture plate and counted with a haemocytometer. 50 µL cell suspension with 10^4 cells was dropped onto each scaffold to allow cells attachment on the scaffold surface (Figure 3.8), they were cultured at 37 °C in a 5% CO_2 humidified environment for 1 hour. After 1 hour, 1 mL medium was added on each well. Culture media were changed every day.

3.2.6.3. MTT assay for cell viability

Bone marrow stem cells (BMSCs) cell proliferation and viability on the scaffolds' surfaces were quantitatively evaluated via MTT assay (Invitrogen Life Technologies, Gaithersburg, MD). The assay is dependent on the cellular reduction of MTT (3-(4,5-dimethylthialzol-2-yl)-2,5-diphenyltetrazolium bromide), by the mitochondrial dehydrogenase enzymes of viable cells, to a blue formazan product which can be measured by spectrophotometer (Suslu, Albayrak, Urkmez, Bayir, & Cocen 2014). The quantity of purple formazan crystals formation is proportional to the amount of viable cells. 1., 3., and 5. days after cell seeding, culture medium from each well was aspirated and taken the place of 50 µl per well of MTT solution and 450 µl DMEM

(serum free) for each scaffold in 24-well culture plates. The plate was incubated for 2 hours at 37 °C. The media were aspirated and the cells were then lysed using 500 µL per well of dimethyl sulfoxide (Sigma Aldrich, St. Louis, USA) to release and solubilize formazan crystals. After 15 minutes of rotary agitation, DMSO solution, which contained formazan crystals, was separated into 96-well-plates as 100 µL to read absorbance at 540 nm. UV/Visible spectrophotometer (Molecular Devices-Versa Max) was used for measurement of absorbance. Amount of viable cell that correlated with absorbance was determined via calibration curve as a cell number.

3.2.7. Simulated body fluid

Simulated body fluid (SBF) is used to simulate physiological body condition and biological mineralization. The standard procedure of Tas was performed to prepare SBF. The solution is prepared by dissolving given quantities of chemicals for 1 litre. 1000 ml capacity glass beaker is filled with 700 ml high purity deionized water. Bottle is placed on a magnetic stirrer. Starting from the NaCl, reagents are added by one by in the following order with Table 3.1. Each reagent was completely dissolved by using magnetic stirring rod. 15 ml HCl is added before the addition of sixth reagent. After addition of eight reagent, temperature of solution increased from ambient temperature 37Cº.Then the solution is titrated with HCl to adjust pH to 7.4 at 37ºC. During the titration, deionize water is controlledly added to make the final volume 1 mL. It is important to have clear solution. The bottle is tightly capped and kept in a refrigerator at +4º and can be stored for a month.

Table 3.1 : Chemical composition of simulated body fluid (Tas 2000).

Order	Reagent	Amount (gpl)
1	NaCl	6.547
2	NaHCO3	2.268
3	KCl	0.373
4	Na2HPO4.2H2O	0.178
5	MgCl2.6HO	0.305
6	CaCl2.2H2O	0.368
7	Na2SO4	0.071
8	(CH2OH)3CNH2	6.057

3D printed samples were soaked in 5 ml SBF in 6 well plate for 2 weeks. Samples were placed in an incubator at 37°C to simulate the human body. Then, SBF solution was changed twice per week to maintain consistent pH.

3.2.8. Scanning electron microscopy

The media were aspirated from culture plate wells after cell culture for 5 days. Samples were washed with physiological saline solution for 30 seconds. Following that the samples were soaked in 5% glutaraldehyde containing 0.1M sodium cocadylate (Sigma Chemical Company, St. Louis, USA) buffer for 30 minutes. Then, this solution was replaced by 7% sucrose containing 0.1 M sodium cocadylate for 30 minutes (without any washing step). After that this solution was replaced by 2% osmium tetroxide containing 0.1 M sodium cocadylate for 30 minutes (without any washing step). Next, samples were washed with deionized (DI) water for 5 minutes and this step was repeated. Following washing step, the samples underwent gradual dehydration in an ethanol series of 35%, 50%, 70%, 85%, 95%, 100% and 100% for 5 minutes for each steps. Finally, samples were placed in hexamethyldisilazane (Sigma Aldrich, St. Louis, USA) for 5 minutes, allowed to dry overnight, and stored in a desiccator. Samples were sputter-coated with gold–palladium prior to imaging. The surface morphologies of samples were investigated through scanning electron microscope (FEI Quanta FEG 250). Observations were conducted at an accelerating voltage of 4 kV.

3.2.9. Statistical analysis

ANOVA two way analysis of variance and student t-test were performed to determine the statistical significance between experimental groups. N=3 for each group in all experiments. Mechanical results are described as means ± standard deviation (SD). A value of $p<0.05$ rejects null hypothesis and was considered to be statistically significant.

4. RESULTS AND DISCUSSION

4.1. Manufacturing

Since ceramic materials have high solubility especially in biological fluids, manufactured samples were sintered at 1150 °C for 2 hours to reduce dissolution ratio. In the same manner, Fielding et al. sintered 3D printed TCP based scaffolds in 1250 °C for 2 hours (Fielding et al. 2012). And also Bergman et al. sintered 3D printed β-TCP and BGH glass mixture at 1000 °C (Bergmann et al. 2010). For our samples sintering temperature was calculated from literature date which mention in materials and methods section. Sintering temperature should be between tamman temperature and melting temperature of material ($T_{melting} > T_{sintering} > T_{tamman}$) (Iribarne 1997).

It is clearly seen that when non-sintered sample is immerse in PBS, it starts to dissolve in high rate and nearly 1/3 of the sample was at the bottom of the glass in a matter of minutes Figure 4.1(a). However, sintered samples highly stand up to dissolution. Sintered sample was soaked in PBS for 1 week and there is no visible dissolution Figure 4.1(b).

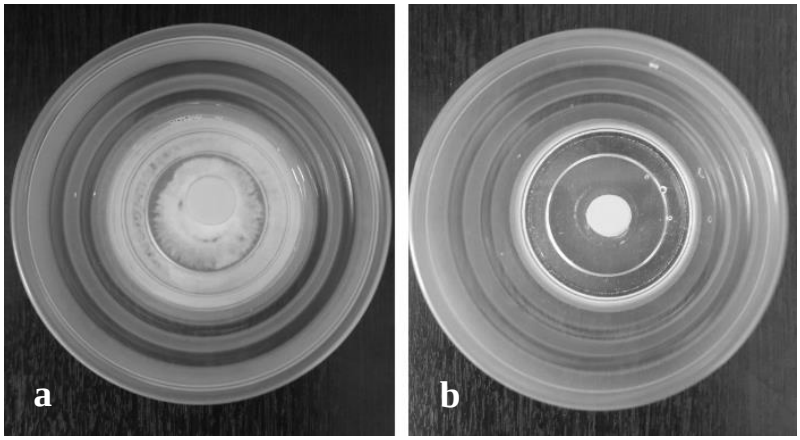

Figure 4.1 : Comparison of dissolution, a. non-sintered 3D printed sample in PBS, b. sintered 3D printed sample in PBS.

While 500 µm, 750 µm and 1000 µm pore sized scaffolds were manufactured it was seen that 500 µm pores could not be open by using depowdering after printing

process. Although 3D printer has high resolution, removing loose powder is critical step. Thus, 750 µm and 1000 µm pore sized scaffolds were more producible. In addition to this, scaffold pore intensity was another parameter which affects the solubility.

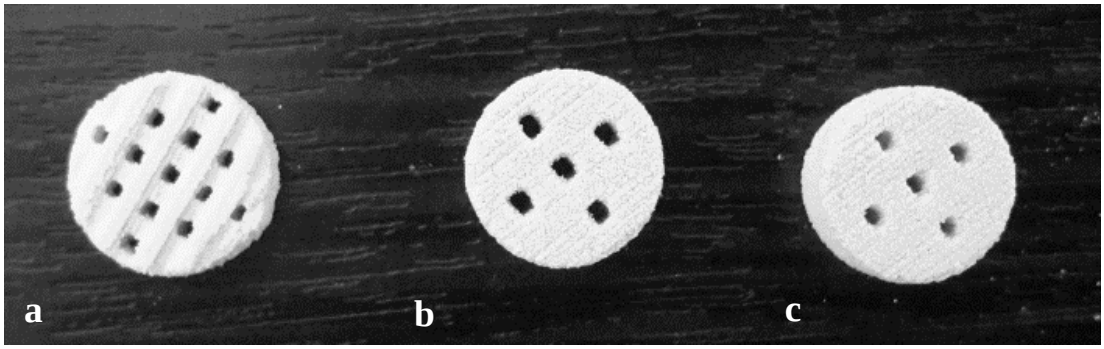

Figure 4.2 : Interconnected porous scaffold design a. High number of 750 µm pores (relatively), b. Lower number of 1000 µm pores (relatively), c. Lower number of 750 µm pores (relatively).

Figure 4.2 b and c has lower visible solubility than a. Thus, it could be concluded than lower porosity means lower solubility for scaffold design.

4.2. Analysis

4.2.1. Wettability measurements

To observe the hydrophilic character of 3D printed samples wettability measurements were performed. Complete resorption of dropped liquid is an indicator of hydrophilicity. In our measurement, contact angle of samples cannot be measured, so it can be concluded that 3D printed material showed super-hydrophilic property. In the other words, dropped pure water was completely absorbed by the surface of the material.

Biocompatibility of materials is mostly about the cell behaviour when contact with the material and surface characteristics have an important role on cell adhesion. Cell attachment and spreading is the first step of cell-material interaction and its success will highly effect on cell proliferation (Anselme 2000). Cells can attach and grow more easily on hydrophilic surfaces in comparison with hydrophobic surfaces (Yamada et al. 1990). Thus, it can be concluded that our material have convenient surface property in terms of hydrophilicity.

4.2.2. X-ray diffraction (XRD) analysis

XRD analysis of the commercial powder material is performed to detect initial phase of the material and compare it with printed and sintered phases. Before sample fabrication, purchased powder examined by using XRD and its specific patterns demonstrated that commercial powder consisted of calcium hemihydrate ($CaSO_4$. (1/2)H2O) (Figure 4.3). Calcium sulfate hemihydrate (CSHH) is an inorganic compound and also known as plaster of Paris and bassanite. It has been widely used in bone regeneration more than 100 years (Beuerlein & Mckee 2010).

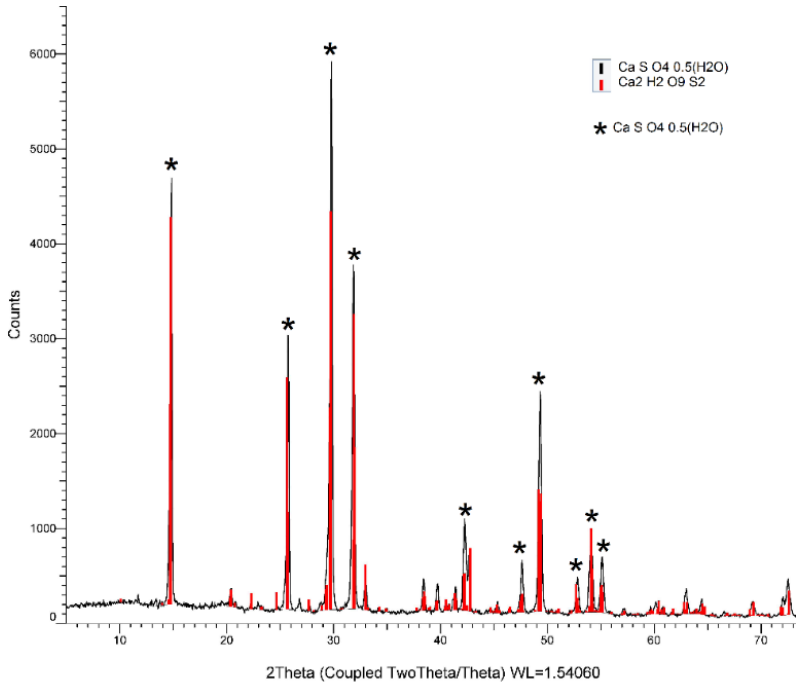

Figure 4.3 : XRD standard patterns for commercial powder (Ca_2SO_4.1/2H_2O).

Following the raw powder, material phases was observed after fabrication. Printed samples were pestle till to have fine particles for XRD analysis. According to specific XRD patterns, powder consisted of gypsum (Ca_2SO_4.2H_2O) after printing process (Figure 4.4). Gypsum specific peaks are shown with + symbol on the graph.

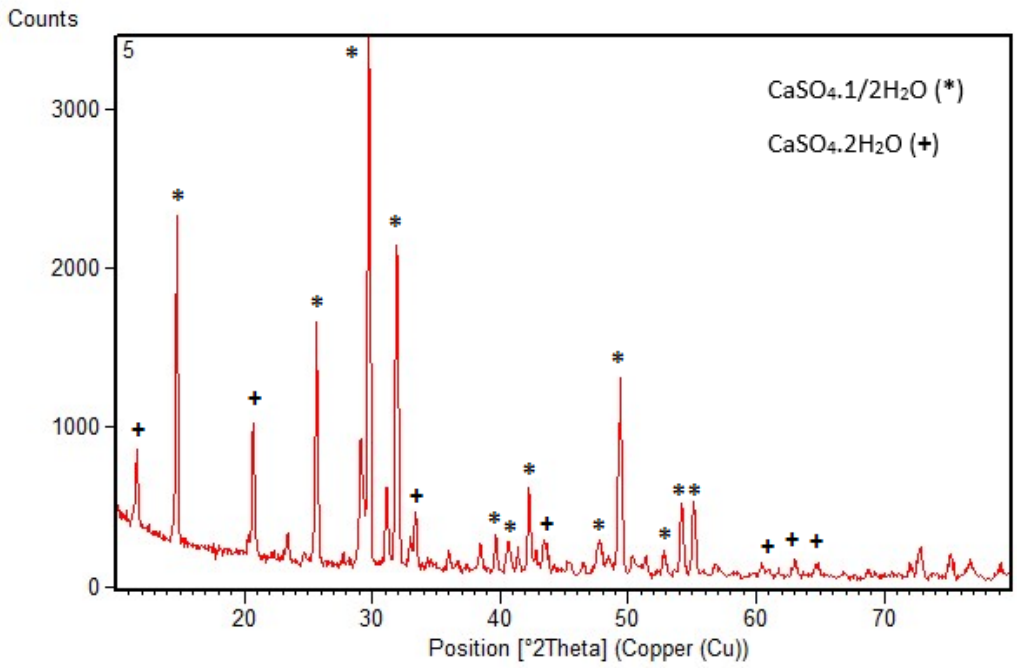

Figure 4.4 : XRD standard patterns for 3D printed commercial powder ($CaSO_4.2H_2O$).

CSHH is produced by heating of gypsum and loses three quarters of water (Coetzee 1980).

$$CaSO_4 . 2H_2O \xrightarrow{Heat} CaSO_4 . {}^{1}/_{2}\ H_2O + {}^{3}/_{2}\ H_2O \qquad \textbf{(1)}$$

If CSHH is mixed with water, the mixture will solidify and the reaction will be reverse;

$$CaSO_4 . {}^{1}/_{2}\ H_2O + {}^{3}/_{2}\ H_2O \longrightarrow CaSO_4 . 2H_2O \qquad \textbf{(3)}$$

Since the binder of 3D printer (2-pyrollidone) have 98% water content, reverse reaction occurred and initial powder CSHH transformed into gypsum after printing process.

Finally, 3D printed and sintered powder was examined with XRD spectroscopy. Specific peaks of the material is match with anhydrite ($CaSO_4$) after sintering process (Figure 4.5).

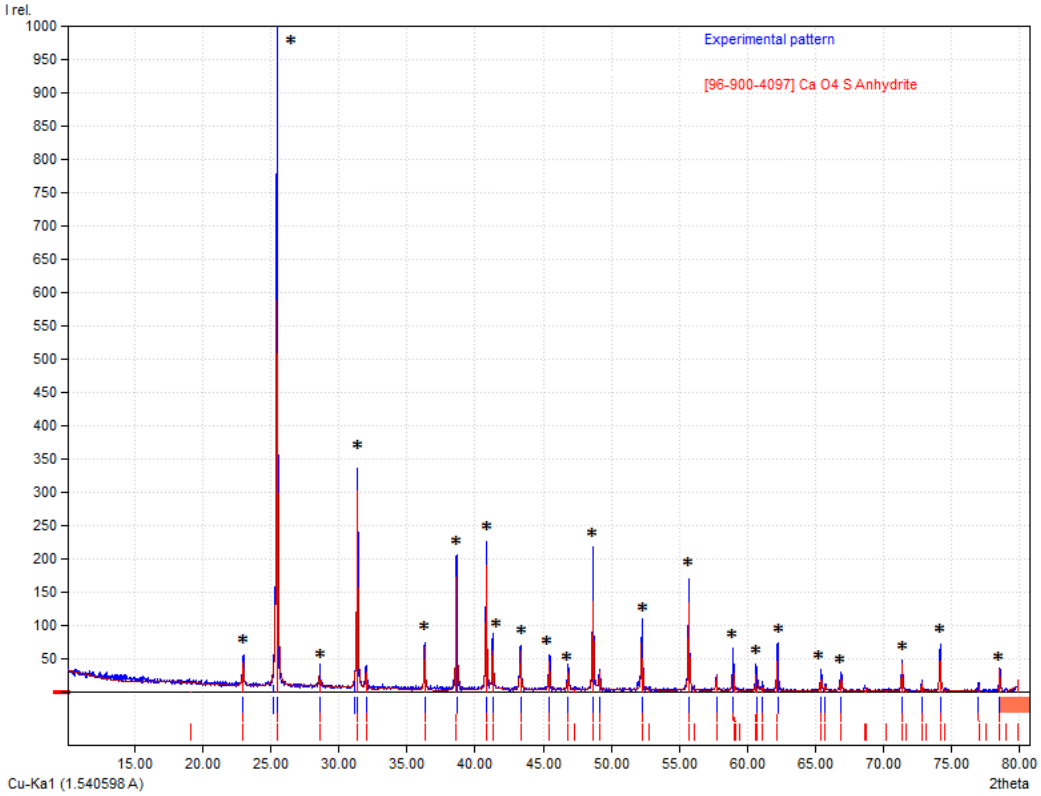

Figure 4.5 : XRD standard patterns for 3D printed, sintered commercial powder ($CaSO_4$).

Sintering was applied under 1150 °C for two hour. Since gypsium transform into anhydrite form above 200 °C, sintered samples were in anhydrite phase.

$$CaSO_4 . 2H_2O \xrightarrow{Heat} CaSO_4 + 2\,H_2O \qquad (2)$$

4.2.3. Thermogravimetric analysis (TGA)

TGA profiles for control, 0.1 wt% ZnO, 0.3 wt% ZnO and 0.5 wt% ZnO samples are given in Figure 4.6 and Figure 4.7. The involved TGA data were summed up in Table 10. According to the data in table 10, the thermal degradation of control and ZnO doped samples is divided into two stages, one small and one main stage. The initial degradation, the main maximum degradation, and the final degradation rate temperatures for control sample was obtained to be about 357, 975, and 1550 °C, respectively.

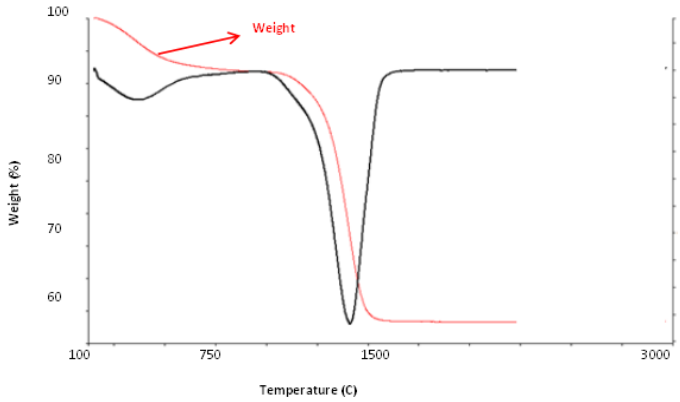

Figure 4.6 : TGA profile for control sample.

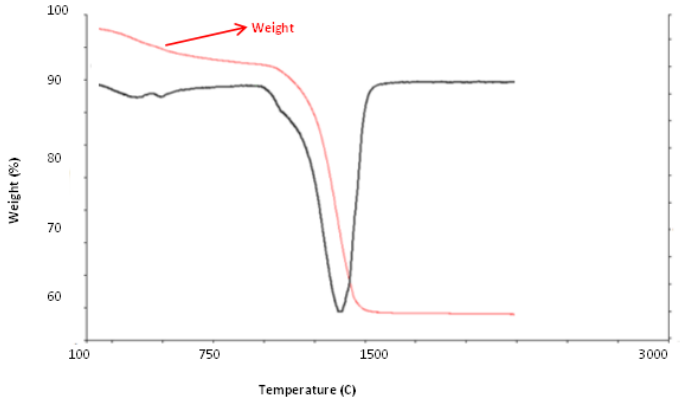

Figure 4.7 : TGA profile for 0.1 wt% ZnO doped sample.

As can be seen in Table 4.1, the main maximum degradation rate temperature for ZnO doped samples was about 976 °C, respectively. Addition of ZnO (0.1%, 0.3% and 0.5%) did not considerably change the maximum degradation temperature of the samples.

Table 4.1 : TGA data for the samples.

Samples	Weight loss to 1800°C %	Initial decomposition temperature (°C)	Maximum decomposition temperature (°C)	Final decomposition temperature (°C)
Control	44	357	975	1550
0.1 wt% ZnO	45	359	976	1552
0.3 wt% ZnO	43	358	978	1551
0.5 wt% ZnO	44	359	978	1550

4.2.4. Thermomechanical analysis (TMA)

Typical sample of dimensional change behaviour of CSHH material with temperature for the first and second heating cycle is given in Figure 4.8. Reheating of specimens immediately after cooling from the first heating cycle resulted in steady and near-linear changes in the thermal expansion curve.

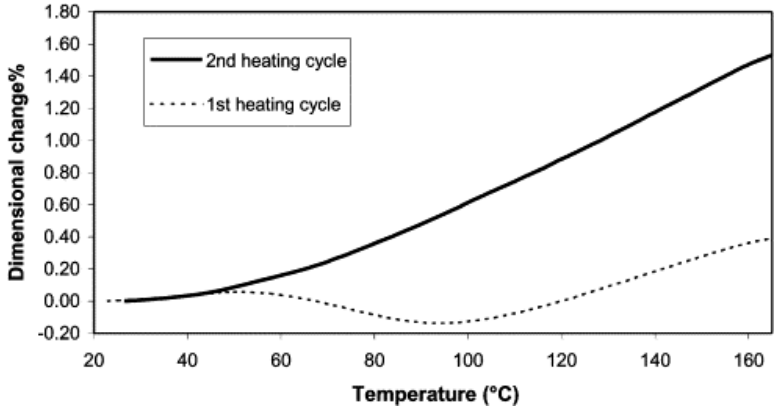

Figure 4.8 : Typical graph showing the percentage of dimensional change with temperature.

Figure 4.9 plots the relative change in sample length (ΔL/L0) along the X-direction as a function of temperature for control sample. Both the second heating and the second cooling ramps are included in the plot.

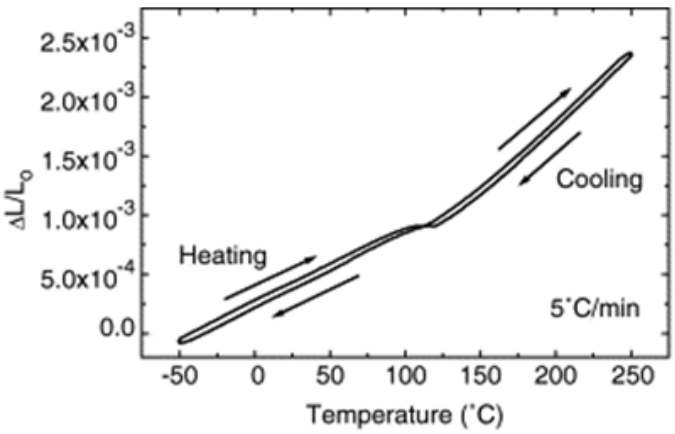

Figure 4.9 : Relative change in sample length along the X-direction as a function of temperature obtained by TMA.

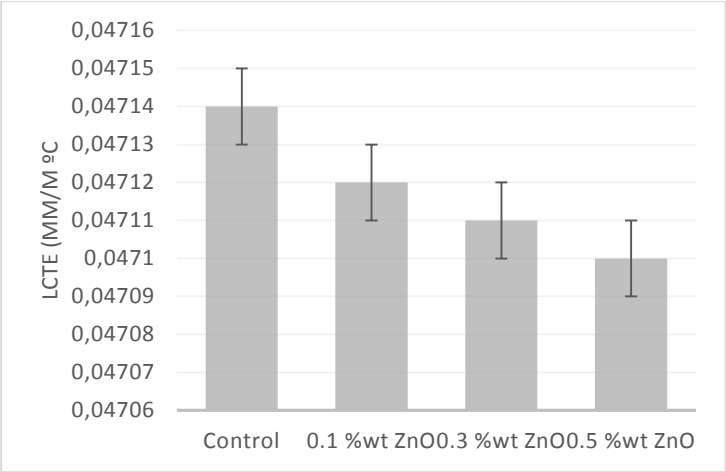

Figure 4.10 : LCTE values of control and ZnO doped samples.

The results of the measurements according to control and ZnO doped samples, ZnO content displayed in Figure 4.10 give the mean and standard deviation values for the LCTE. It is clear that, LCTE values of the samples decreased with increasing of Zn content up to 0.5%.

4.2.5. Mechanical tests

Compression tests of zinc doped, 3D printed, and sintered CSHH samples were performed by using Shimadzu Autograph AG-IC Series universal testing machine to evaluate mechanical properties. 0; 0.1; 0.3 and 0.5 wt% ZnO included cylindrical (diameter of 10 mm and the height of 10 mm) CSHH samples were processed under the same conditions. Three samples for each group is tested and F (load), Δh (height change) values were recorded and the stress and strain values were calculated.

Table 4.2 shows the calculated young's modulus, max force and compression strength for each group. Standard mean and mean values were calculated and tabulated in the table. Calculated values were graphed for better understanding (Figure 4.11). It was found that the doped samples showed greatest compressive strength than pure CSHH. The Young's modulus values of control, 0.1 wt%, 0.3 wt% and 0.5 wt% Zn including groups were calculated as 35.39 ± 3.12 MPa, 58.23 ± 2.13 MPa, 65.04 ± 1.82 MPa, and 98.78 ± 3.44 MPa respectively. Moreover, compressive strength of the four different samples showed a similar increasing trend by the addition of Zn as Young's modulus. Compressive strengths of the samples were calculated as 0.87 ± 0.04 MPa, 0.90 ± 0.09 MPa, 1.18 ± 0.01 MPa and 2.48 ± 0.04

MPa respectively for control, 0.1 wt%, 0.3 wt% and 0.5 wt% Zn including groups. While, there is statistically difference with each group in Young Modulus, there is not statistically difference for control and 0.1 wt%; 0.1 wt% and 0.3 wt% in compression strength. It is clear that, compressive strength of the samples increased with increasing of Zn content up to 0.5%. The highest values of Young's modulus and compressive strength obtained at 0.5 % Zn loading (approximately 2.8 and 2.85 times higher than control group in terms of Young's modulus and compressive strength, respectively) while the least values were observed for control groups. The Young's modulus and compressive strength values of all zinc including groups were higher than control group. Thus, it can be concluded that zinc addition increase mechanical strength of CSHH based scaffolds.

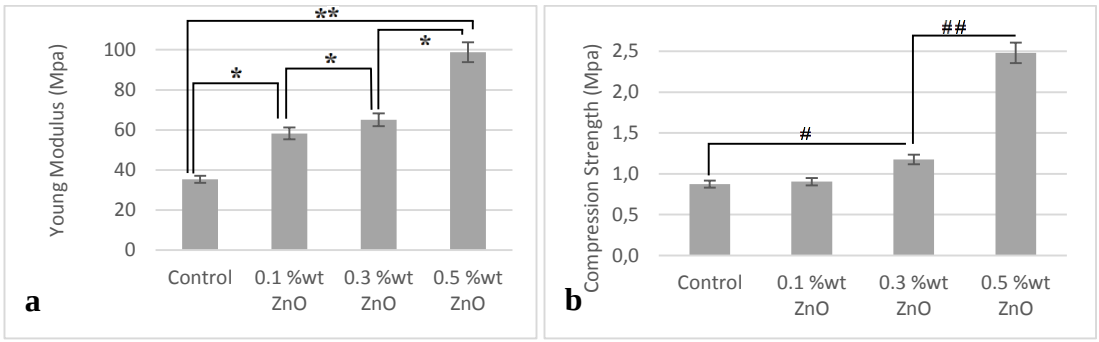

Figure 4.11 : Mechanical test results a. young modulus graph, b. compression strength graph.*,# Statistically significant difference each other (n=3, *p<0.05;**p<0.01; #p<0.05; ##p<0.01).

Table 4.2 : Compression Test Results.

Group	Control			0.1 %wt ZnO			0.3 %wt ZnO			0.5 %wt ZnO		
Sample No	*S1*	*S2*	*S3*	*S1*	*S2*	*S3*	*S1*	*S2*	*S3*	*S1*	*S2*	*S3*
Young Modulus (MPa)	33.12	33.25	39.80	55.59	60.80	58.32	64.46	67.50	63.17	103.63	96.72	95.98
	Mean		*SD.*	*Mean*		*SD.*	*Mean*		*SD.*	*Mean*		*SD.*
	35.39		3.12	58.23		2.13	65.04		1.82	98.78		3.44
Max Force (N)	65.77	66.53	73.53	73.14	61.14	78.81	93.36	92.03	91.78	199.09	195.20	190.50
Compression Strength (MPa)	0.84	0.85	0.94	0.93	0.78	1.00	1.19	1.17	1.17	2.53	2.49	2.43
	Mean		*SD.*	*Mean*		*SD.*	*Mean*		*SD.*	*Mean*		*SD.*
	0.87		0.04	0.90		0.09	1.18		0.01	2.48		0.04

4.2.6. Cell viability

MTT assay was performed using BMSC cell line to investigate material toxicity in terms of cell viability. Reference curve (4.13 (b)) was prepared for BMSC to calculate cell numbers (4.13 (c)) from absorbance values (4.13 (a)). MTT results showed that there is a clear difference between pure and zinc doped CSHH (4.13 (c)). The amount of cells was significantly greater in doped samples than pure ones. While 0.1 wt% zinc doping increased cell proliferation approximately 100%, there was around 150% increase in cell viability with the highest level at 0.5 wt% zinc. It is clear from the bar graph (4.13 (d)) that cell viability rose with the increase in Zn concentration for each time period. Beside it has no toxic effect on cells, Zn shows a positive impact on cell proliferation. Furthermore, this positive influence was supported by SEM images in which cells represent a complete attachment on surfaces of samples as will be discussed in the following section.

4.2.7. Scanning electron microscopy

Scanning electron microscopy (SEM) observation was done for microstructural analysis of samples to investigate;

- Effect of sintering process on ceramic particles,
- Apatite formation on pure and zinc doped CSHH samples,
- Cell attachment on pure and zinc doped CSHH samples.

Firstly, sintering is the process of compacting solid particles by heat or pressure without melting.

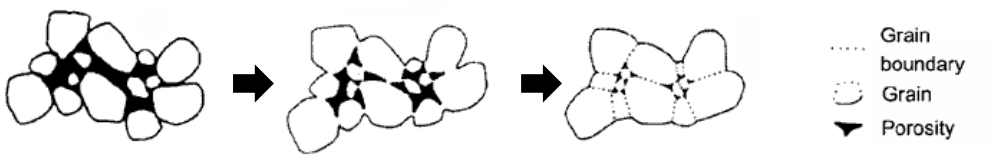

Figure 4.12 : Grain shape changes during sintering process (retrieved from www.keramverband.de, 2016).

Some ceramics have lower affinity for water and they dissolve easily in body fluids. Sintering reduced dissolubility in addition the results in reduction in porosity and increase in mechanical strength of parts. This process results in a volume reduction; this is called sintering shrinkage (Figure 3.3 (g)). As it can be clearly seen from

Figure 4.12, grains are fused together by reduction in porosity. Similarly, while in the Figure 4.14(a) particles are piece by piece, they appear like an integrated unit after sintering processes Figure 4.14(b). SEM results confirmed the data gathered from dissolution test (Figure 4.1) and length comparison in the Figure 3.3 (g).

Another parameter which analysed from SEM observations was effect of zinc on apatite formation. When bioactive ceramics such as hydroxyapatite placed in body, they bond to bone and increase healing time promoting by bone formation. Bone-like apatite surface could be created in vitro by using SBF which simulates human plasma to check apatite formation potential of material. If the materials could form apatite crystals on their surface, it is tough as a promising material for bone-bonding and bioactivity (Jonasova, Muller, Helebrant, Strnad, & Greil 2004).

Kanzaki et al. researched the inhibitory effect of zinc on hydroxyapatite formation. Although zinc promote bone formation by simulating bone cell which produce HA and have a positive effect on HA increase circuitously, zinc by itself inhibits apatite growth due to structural mismatch with grown layer (Ito 2002; Kanzaki 2000). SEM micrographs illustrates surface microstructure of pure CSHH after being treated in 2 weeks in SBF in the (4.15(a)(b)). The apatite coated surface was shown by arrows. The pure CSHH had more apatite in comparison with zinc doped sample (4.15 (c)(d). Negative influence of zinc on apatite formation reduced the intensity of crystals.

Finally, bone marrow stem cell (BMSC) adhesion on pure and zinc mixed CSHH matrix was examined. BMSCs was attach and spread on CSHH surface properly. Anchor points of cells were clearly seen from Figure 4.16 (b). It was important that dopants do not compromise the biocompatibility of CSHH. Cell spreading is key function which describes the adherence of cell to the substrate to provide cell proliferation and matrix formation. Since the cells move to proliferation phase after satisfying attachment was provided, if cells do not spread enough and have a round shape, they do not survive anymore (Paul & Sharma 2007). Since zinc do not have a negative effect on cell attachment, BMSCs spread out, occupied as much surface area as possible. All zinc doped groups have flattened morphology on ceramic samples at the end of the 5^{th} day. All samples showed good bioactivity and spreading (Figure 4.17, Figure 4.18, Figure 4.19). These micrographs confirms the data gathered from MTT.

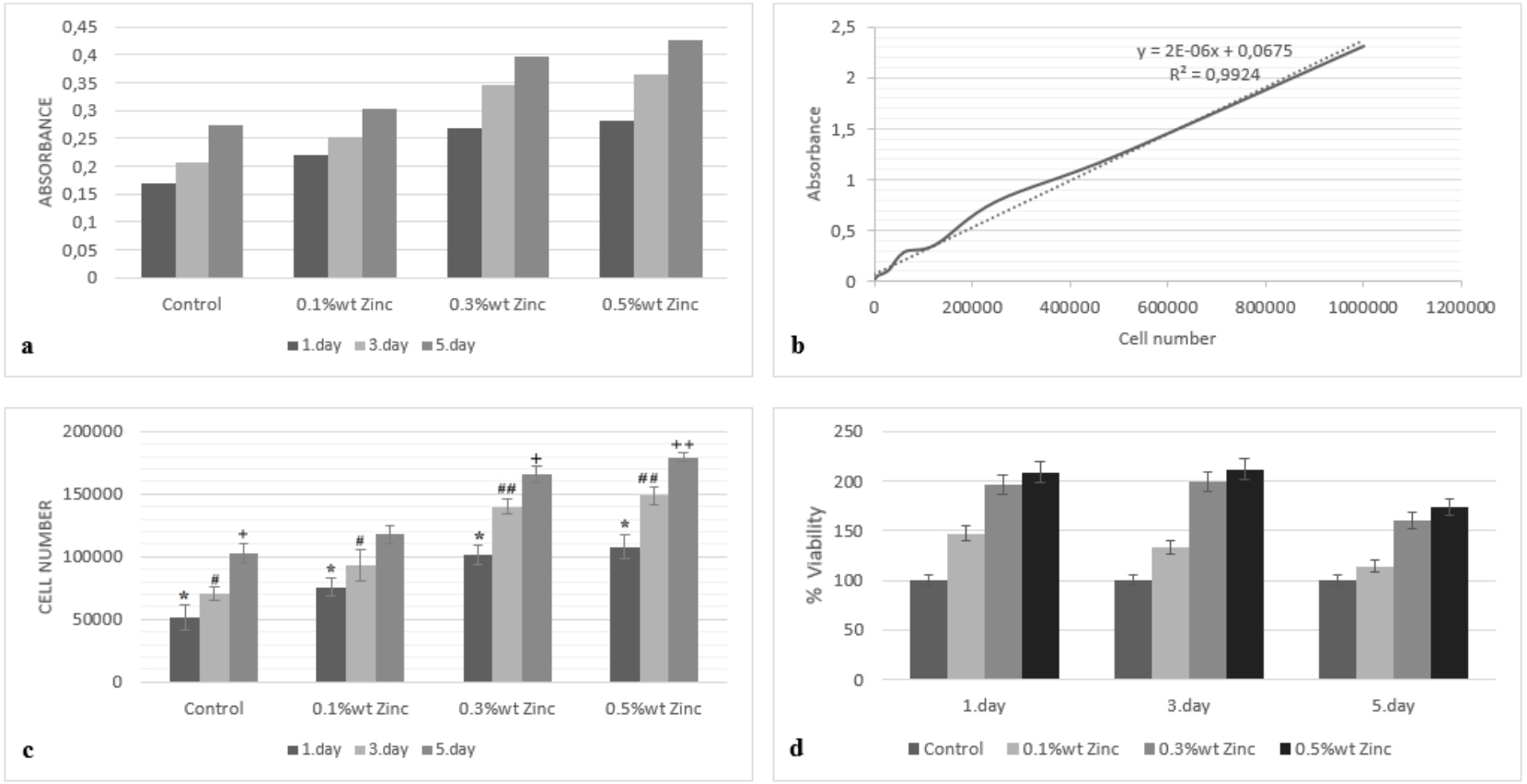

Figure 4.13 : a. MTT test absorbance values for each group at 1., 3., and 5. Days, b. Growth curve (reference curve) of BMSC cell line, c. Cell number values calculated by using reference curve, d. cell viability ratio zinc doped groups (compared with control). *,#.+ Statistically significant difference between control and each (n=3, *p<0.01; #p <0.05; ##p <0.01; +p <0.05; ++p <0.01).

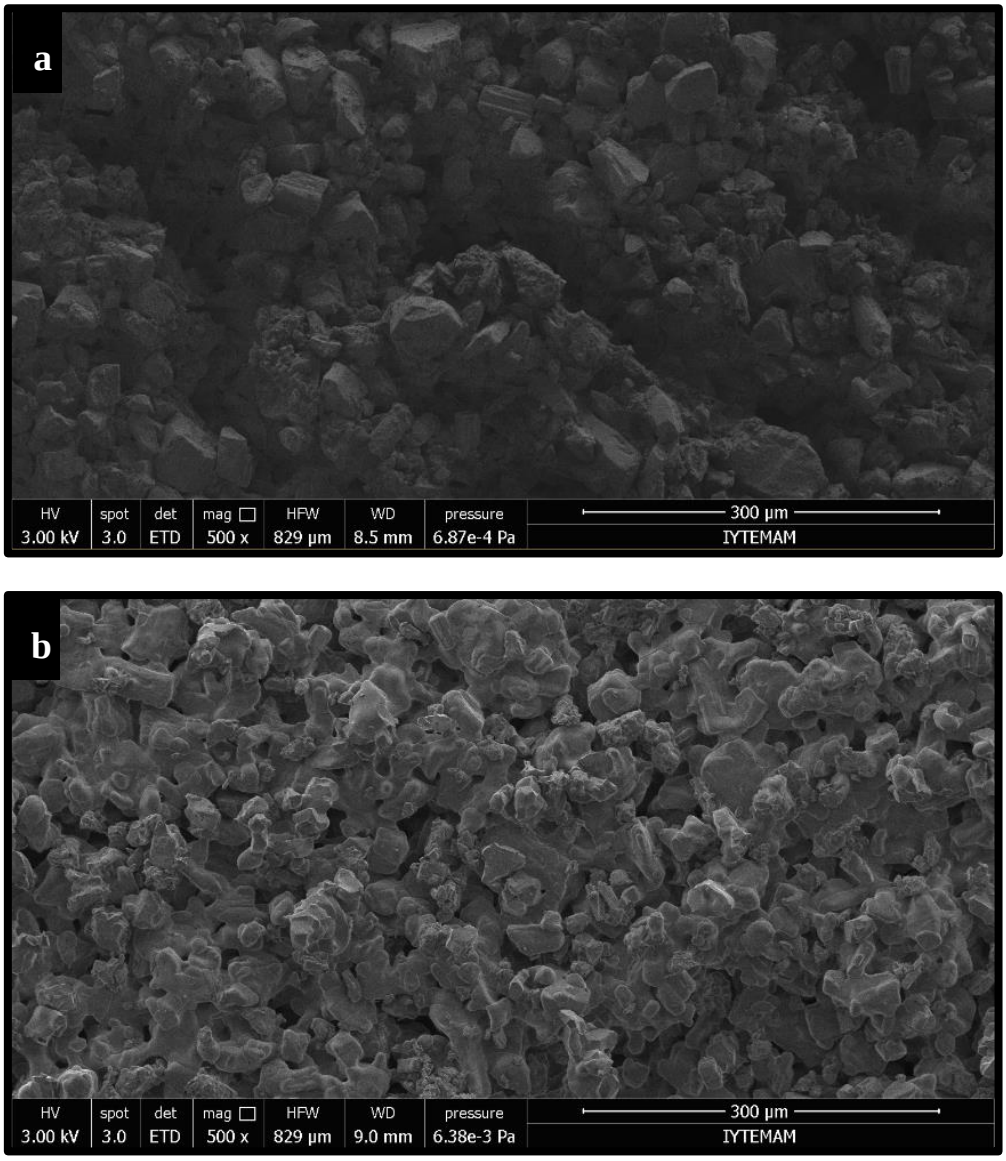

Figure 4.14 : SEM micrographs illustrating surface microstructure of 3D printed a.Green, b. Sintered samples.

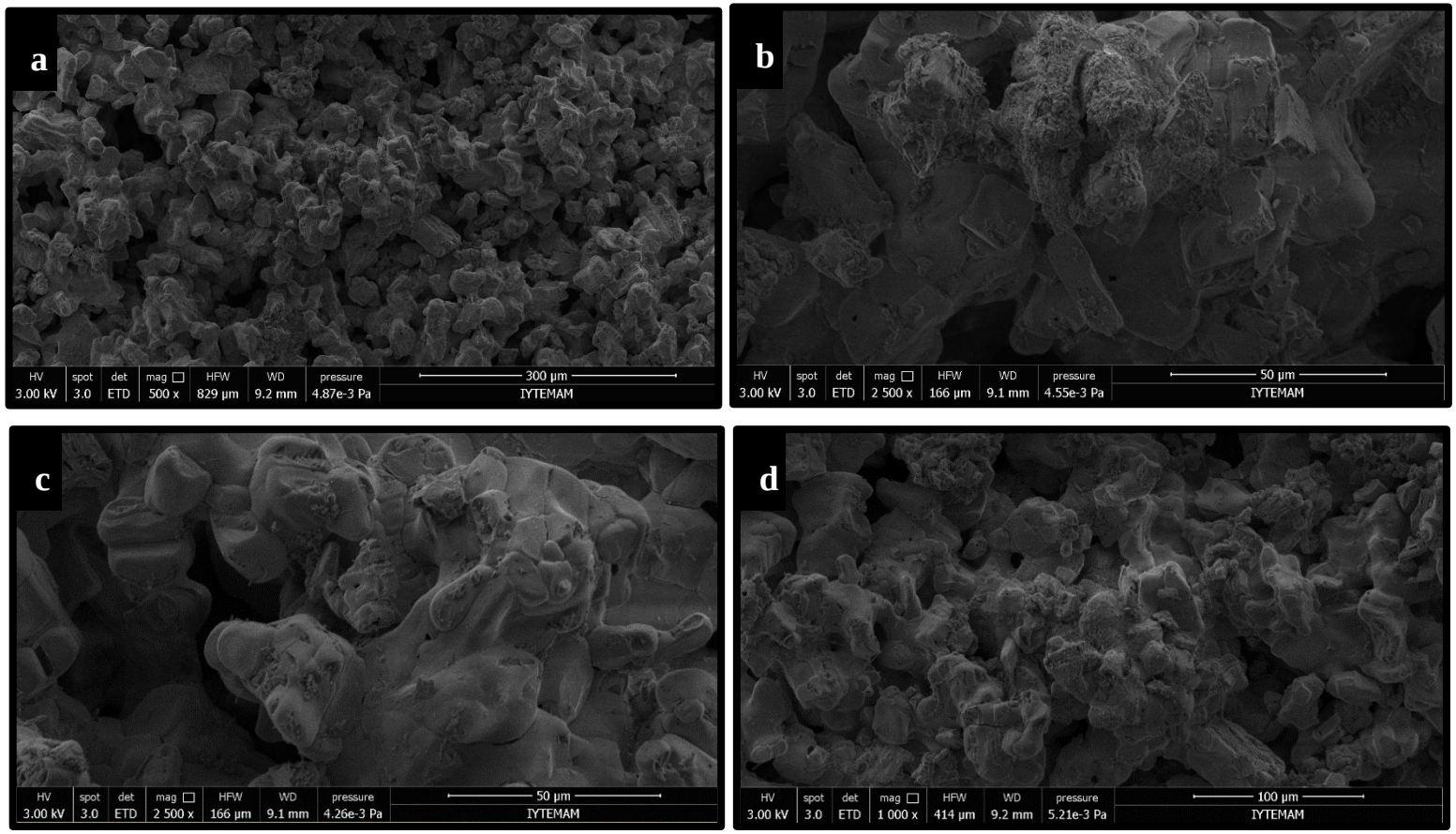

Figure 4.15 : SEM micrographs illustrating surface microstructure of a. pure CSHH after being treated in 2 weeks in SBF 100µm resolution, b.50µm resolution, c.0.3 wt% ZnO containing CSHH after being treated in 2 weeks in SBF b.300µm resolution, c.50µm resolution.

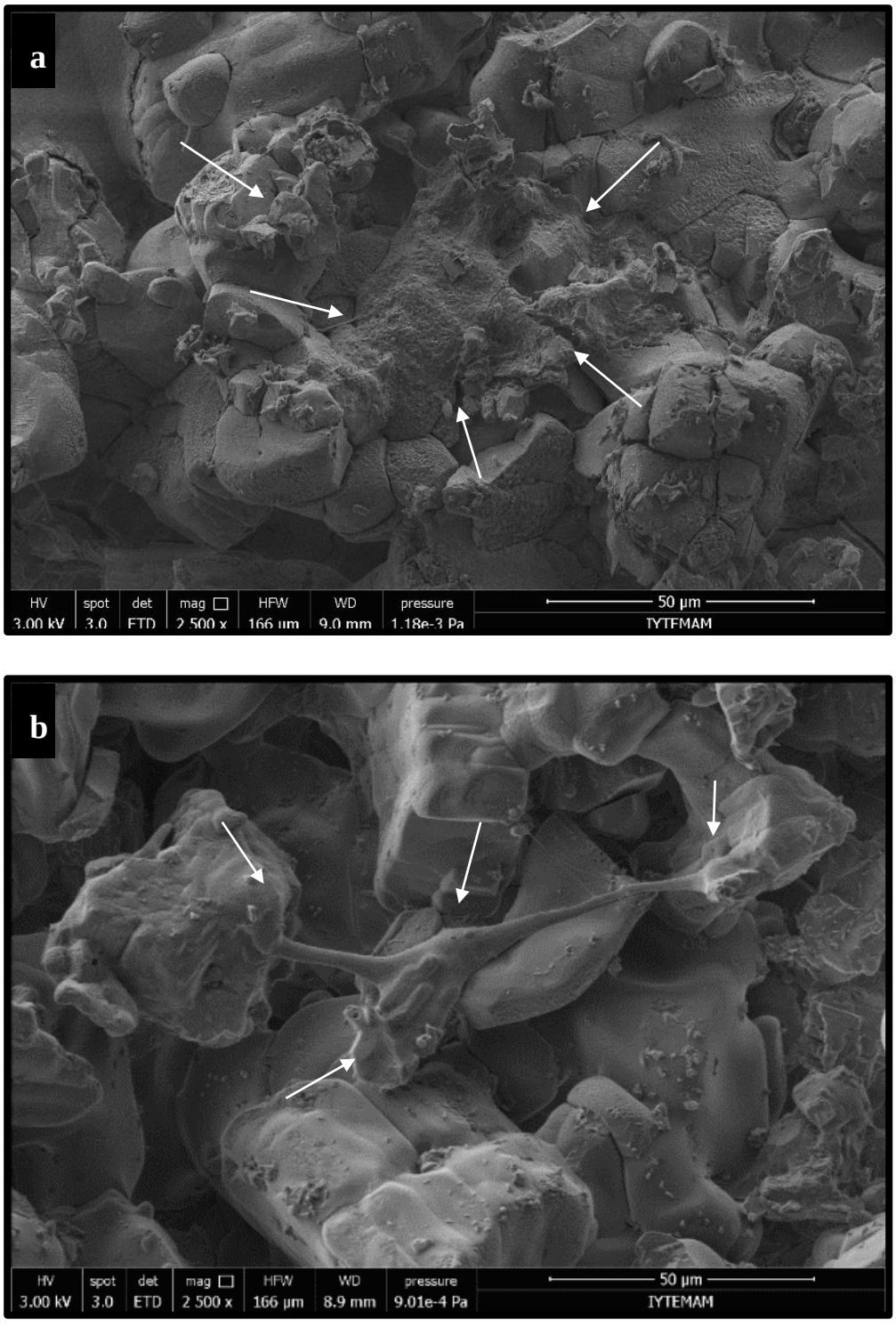

Figure 4.16 : SEM micrographs of BMSCs showing the cell adhesion morphology on the pure CSHH scaffold surface at 5th day from different zones a. spread, flattened BMSC, b. attaching and anchor points of BMSC (arrows shows cells).

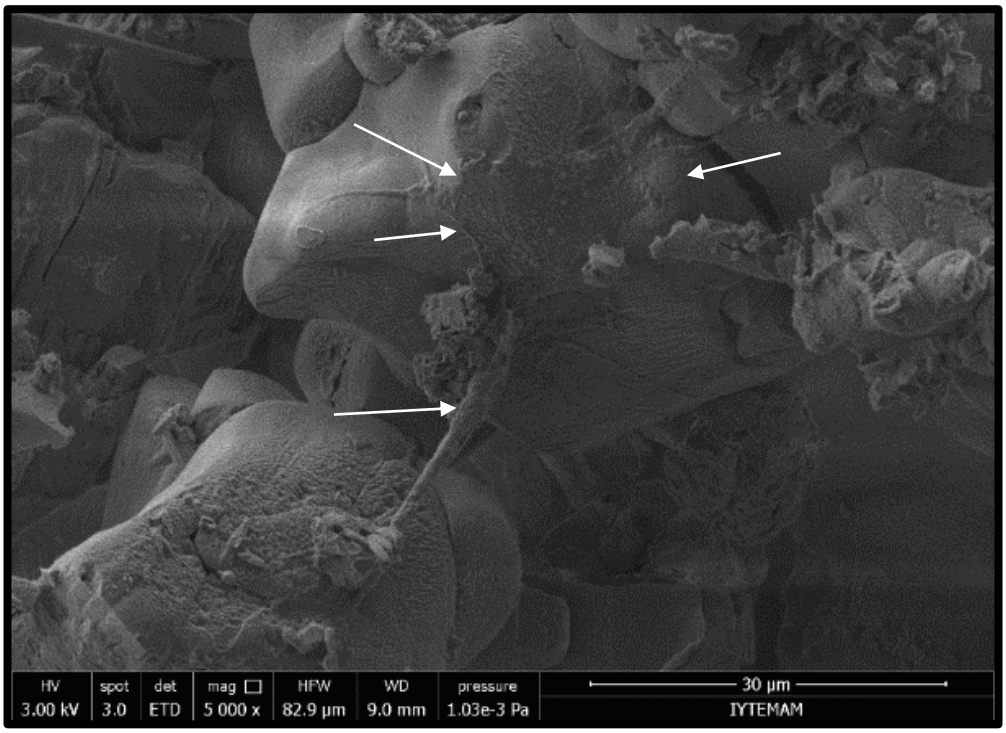

Figure 4.17 : SEM micrographs of BMSCs showing the cell adhesion morphology on the 0.1 wt% ZnO doped CSHH scaffold surface at 5th day (arrows shows cells).

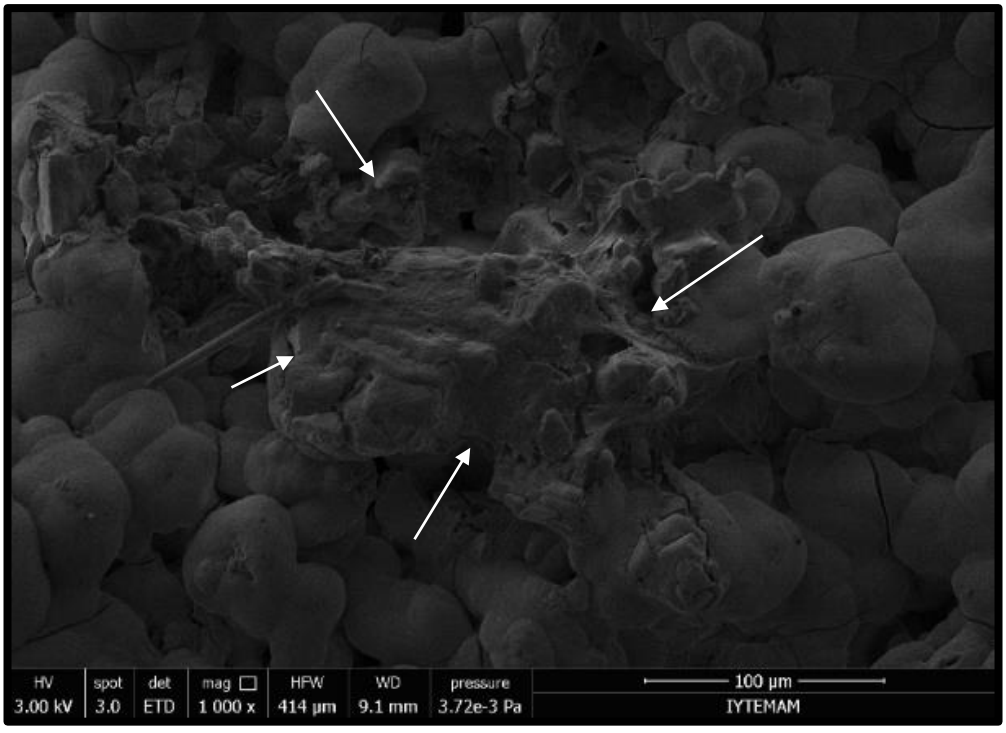

Figure 4.18 : SEM micrographs of BMSCs showing the cell adhesion morphology on the 0.3 wt% ZnO doped CSHH scaffold surface at 5th day (arrows shows cells).

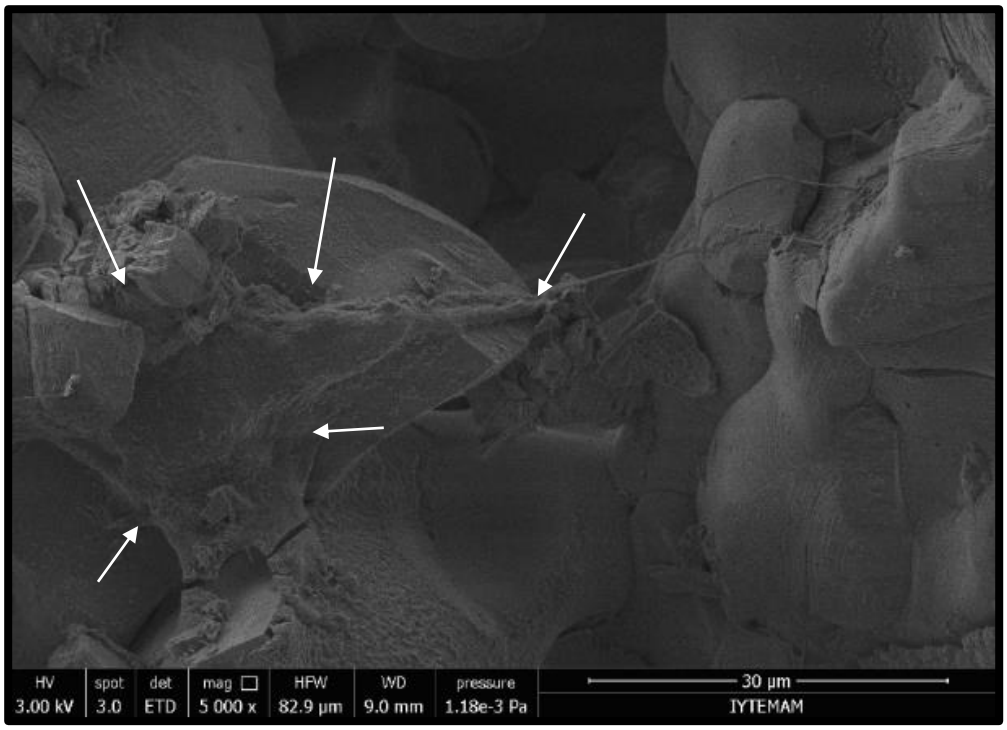

Figure 4.19 : SEM micrographs of BMSCs showing the cell adhesion morphology on the 0.5 wt% ZnO doped CSHH scaffold surface at 5th day (arrows shows cells).

5. CONCLUSIONS

Pure and zinc doped, commercially purchased powder based ceramic scaffolds were manufactured by using powder based 3D printer. These samples were then tested for physical, mechanical, and biological properties to investigate the usage potential of the material in personalized scaffold fabrication processes.

Since CSHH is a hydrophilic material, contact angle measured as zero. XRD results validated that our powder is calcium sulfate hemihydrate ($CaSO_4.1/2H_2O$). Since the binder of 3D printer (2-pyrollidone) have 98% water content, after printing process CSHH transformed into gypsum. After sintering process specific peaks of the material is match with anhydrite ($CaSO_4$) due to water loss at higher temperatures.

Compressive strength of the samples increased with increasing of Zn content up to 0.5%. The highest values of Young's modulus and compressive strength obtained at 0.5 % Zn loading while the least values were observed for control groups. The Young's modulus and compressive strength values of all zinc including groups were higher than control group. Thus, it can be concluded that zinc addition increase mechanical strength of CSHH based scaffolds.

According to biocompatibility results, samples did not show any negative and toxic effect from day 1 to day 5. The ceramic material demonstrates the capacity for cell attachment and potential for cell growth. The proliferation of BMSCs were significantly increased compared with those on the control according to MTT results.

Since zinc do not have a negative effect on cell attachment, BMSCs spread out, occupied as much surface area as possible. All zinc groups have flattened morphology on ceramic samples at the end of the 5^{th} day. All samples showed good bioactivity and spreading

This study demonstrated successful combination of CSHH, zinc and 3DP to create biocompatible bone grafts. As a consequence, 3D printed zinc doped CSHH is a promising for tissue engineering on custom artificial scaffold applications.

6. FUTURE WORK

Non-porous block samples were used in this study to check the feasibility of the 3D printed material in terms of physical, mechanical and biological properties. However, 500µm, 750µm and 1000µm pore included scaffolds were optimized about design issue, produced and the cultured to control if they were dissolved or not. In following studies porous scaffolds will be used.

Secondly, non-invasive image based 3D models such as CT images will be used to design and produce defect match scaffolds. In this way, it will enable our materials to be used as bone substitute in tailored bone scaffolds.

Another issue is that, scaffolds will be doped with different type of dopants such as silica and magnesium to increase mechanical properties. The advantages of other trace elements will be investigated.

BMCS cell line was used in this study to investigate the biocompatibility of material. In the following studies BMSC will be differentiate to bone cells by using additional stimuluses.

BMSC seeded CSHH scaffolds will be cultured a bioreactor. Thus, a complete 3D printed CSHH sample with osteoblast cells may form a strengthened calcified bone fragment.

REFERENCES

al Ruhaimi, K. A. (2001). Effect of calcium sulphate on the rate of osteogenesis in distracted bone. *Int J Oral Maxillofac Surg, 30*(3), 228-233. doi: 10.1054/ijom.2001.0048

Alhava, E. M., Olkkonen, H., Puittinen, J., & Nokso-Koivisto, V. M. (1977). Zinc content of human cancellous bone. *Acta Orthop Scand, 48*(1), 1-4.

Anselme, K. (2000). Osteoblast adhesion on biomaterials. *Biomaterials, 21*(7), 667-681.

Asadi-Eydivand, M., Solati-Hashjin, M., Farzad, A., & Abu Osman, N. A. (2016). Effect of technical parameters on porous structure and strength of 3D printed calcium sulfate prototypes. *Robotics and Computer-Integrated Manufacturing, 37*, 57-67. doi: 10.1016/j.rcim.2015.06.005

Bandyopadhyay, A. B., S.; Xue, W.; Bose, S. (2006). Calcium Phosphate-Based Resorbable Ceramics: Influence of MgO, ZnO, and SiO2 Dopants. *Journal of the American Ceramic Society, 89*(9).

Bayraktar, D. T., C. (1999). Chemical Preparation of Carbonated Calcium Hydroxyapatite Powders at 37 ° C in Urea-containing Synthetic Body Fluids. *Journal of the European Ceramic Society, 19*.

Bergmann, C., Lindner, M., Zhang, W., Koczur, K., Kirsten, A., Telle, R., & Fischer, H. (2010). 3D printing of bone substitute implants using calcium phosphate and bioactive glasses. *Journal of the European Ceramic Society, 30*(12), 2563-2567. doi: 10.1016/j.jeurceramsoc.2010.04.037

Beuerlein, M. J. S., & Mckee, M. D. (2010). Calcium Sulfates: What Is the Evidence? *Journal of Orthopaedic Trauma, 24*, S46-S51. doi: 10.1097/BOT.0b013e3181cec48e

Beyersmann, D., & Haase, H. (2001). Functions of zinc in signaling, proliferation and differentiation of mammalian cells. *Biometals, 14*(3-4), 331-341.

Bose, S., Roy, M., & Bandyopadhyay, A. (2012). Recent advances in bone tissue engineering scaffolds. *Trends Biotechnol, 30*(10), 546-554. doi: 10.1016/j.tibtech.2012.07.005

Brydone, A. S., Meek, D., & Maclaine, S. (2010). Bone grafting, orthopaedic biomaterials, and the clinical need for bone engineering. *Proc Inst Mech Eng H, 224*(12), 1329-1343.

Butscher, A. (2013). Powder based three-dimensional printing of calcium phosphate structures for scaffold engineering. (*Doctor of Science*), ETH ZURICH.

Coetzee, A. S. (1980). Regeneration of bone in the presence of calcium sulfate. *Arch Otolaryngol, 106*(7), 405-409.

Domingos, M., Intranuovo, F., Gloria, A., Gristina, R., Ambrosio, L., Bartolo, P. J., & Favia, P. (2013). Improved osteoblast cell affinity on plasma-modified 3-D extruded PCL scaffolds. *Acta Biomater, 9*(4), 5997-6005. doi: 10.1016/j.actbio.2012.12.031

Ducheyne, P. M., M.; Schepers, E. (1999). *An Introduction to Bioceramics* (Vol. 1): World Scientific.

Eslaminejad, M. B., & Faghihi, F. (2011). Mesenchymal Stem Cell-Based Bone Engineering for Bone Regeneration. In D. Eberli (Ed.), *Regenerative Medicine and Tissue Engineering - Cells and Biomaterials* (pp. 663-668).

Faulkner-Jones, A., Greenhough, S., King, J. A., Gardner, J., Courtney, A., & Shu, W. (2013). Development of a valve-based cell printer for the formation of human embryonic stem cell spheroid aggregates. *Biofabrication, 5*(1), 015013. doi: 10.1088/1758-5082/5/1/015013

Fielding, G. A., Bandyopadhyay, A., & Bose, S. (2012). Effects of silica and zinc oxide doping on mechanical and biological properties of 3D printed tricalcium phosphate tissue engineering scaffolds. *Dent Mater, 28*(2), 113-122. doi: 10.1016/j.dental.2011.09.010

Florencio-Silva, R., Sasso, G. R., Sasso-Cerri, E., Simoes, M. J., & Cerri, P. S. (2015). Biology of Bone Tissue: Structure, Function, and Factors That Influence Bone Cells. *Biomed Res Int, 2015*, 421746. doi: 10.1155/2015/421746

Giannoudis, P. V., Dinopoulos, H., & Tsiridis, E. (2005). Bone substitutes: an update. *Injury, 36 Suppl 3*, S20-27. doi: 10.1016/j.injury.2005.07.029

Gibson, I. R., D.; Stucker, B. (2015). *Additive Manufacturing Technologies* (Second ed.): Springer.

Greiner, A., & Wendorff, J. H. (2007). Electrospinning: a fascinating method for the preparation of ultrathin fibers. *Angew Chem Int Ed Engl, 46*(30), 5670-5703. doi: 10.1002/anie.200604646

Hench, L. L. A., Ö. (1999). Bioactive Glasses. In L. L. Hench (Ed.), *An Introduction to Bioceramics*: World Scientific.

Hesaraki, S., Nemati, R., & Nazarian, H. (2009). Physico-chemical and in vitro biological study of zinc-doped calcium sulfate bone substitute. *J Biomed Mater Res B Appl Biomater, 91*(1), 37-45. doi: 10.1002/jbm.b.31371

Hutmacher, D. W., Sittinger, M., & Risbud, M. V. (2004). Scaffold-based tissue engineering: rationale for computer-aided design and solid free-form fabrication systems. *Trends Biotechnol, 22*(7), 354-362. doi: 10.1016/j.tibtech.2004.05.005

Inzana, J. A., Olvera, D., Fuller, S. M., Kelly, J. P., Graeve, O. A., Schwarz, E. M., . . . Awad, H. A. (2014). 3D printing of composite calcium phosphate and collagen scaffolds for bone regeneration. *Biomaterials, 35*(13), 4026-4034. doi: 10.1016/j.biomaterials.2014.01.064

Iribarne, A. P. I. J. V. A. A. J. (1997). Reactivity of calcium sulfate from FBC systems *Fuel, 76*(4).

Ito, A. K., H.; Otsuka, M.; Ikeuchi, M.; Ohgushi, H.; Ishikawa, K.; Onuma, K.; Kanzaki, N.; Sogo, Y.; Ichinose, N. (2002). Zinc-releasing calcium phosphate for stimulating bone formation. *Materials Science and Engineering C, 22*.

Jonasova, L., Muller, F. A., Helebrant, A., Strnad, J., & Greil, P. (2004). Biomimetic apatite formation on chemically treated titanium. *Biomaterials, 25*(7-8), 1187-1194.

Kanzaki, N. O., K.; Treboux, G., Tsutsumi, S.; Ito, A. (2000). Inhibitory Effect of Magnesium and Zinc on Crystallization Kinetics of Hydroxyapatite (0001) Face. *J. Phys. Chem. B, 104*.

Kapinas, K., & Delany, A. M. (2011). MicroRNA biogenesis and regulation of bone remodeling. *Arthritis Res Ther, 13*(3), 220. doi: 10.1186/ar3325

Kawamura, H., Ito, A., Miyakawa, S., Layrolle, P., Ojima, K., Ichinose, N., & Tateishi, T. (2000). Stimulatory effect of zinc-releasing calcium phosphate implant on bone formation in rabbit femora. *J Biomed Mater Res, 50*(2), 184-190.

Kearns, A. E., & Kallmes, D. F. (2008). Osteoporosis primer for the vertebroplasty practitioner: expanding the focus beyond needles and cement. *AJNR Am J Neuroradiol, 29*(10), 1816-1822. doi: 10.3174/ajnr.A1176

Keaveny, T. M., Morgan, E. F., & Yeh, O. C. (2004). BONE MECHANICS *Mechanics of The Human Body*: Mcgraw-Hill.

Khoo, Z. X. T., J. E. M.; Liu, Y.; Chua, C.K.; Yang, S.; An, J.; Leong, K. F.; Yeong, W. Y. (2015). 3D printing of smart materials: A review on recent progresses in 4D printing. *VIRTUAL AND PHYSICAL PROTOTYPING, 10*(3).

Krar, S. F. G., A. (2003). Rapid Prototyping *Exploring Advanced Manufacturing Technologies*: Industrial Press Inc.

Lichte, P., Pape, H. C., Pufe, T., Kobbe, P., & Fischer, H. (2011). Scaffolds for bone healing: concepts, materials and evidence. *Injury, 42*(6), 569-573. doi: 10.1016/j.injury.2011.03.033

Liu, Y., Lim, J., & Teoh, S. H. (2013). Review: development of clinically relevant scaffolds for vascularised bone tissue engineering. *Biotechnol Adv, 31*(5), 688-705. doi: 10.1016/j.biotechadv.2012.10.003

Liu, Y. J., Yang, Z. Y., Tan, L. L., Li, H., & Zhang, Y. Z. (2014). An animal experimental study of porous magnesium scaffold degradation and osteogenesis. *Braz J Med Biol Res, 47*(8), 715-720.

MacDonald, R. S. (2000). The role of zinc in growth and cell proliferation. *J Nutr, 130*(5S Suppl), 1500S-1508S.

Marsh, D. V. U., D. L. (1985). Rate And Diffusional Study Of The Reaction Of Calcium Oxide With Sulfur Dioxide. *Chemical Engineering Science, 40*(3).

Orsini, M., Orsini, G., Benlloch, D., Aranda, J. J., Lazaro, P., Sanz, M., . . . Piattelli, A. (2001). Comparison of calcium sulfate and autogenous bone graft to bioabsorbable membranes plus autogenous bone graft in the treatment

of intrabony periodontal defects: a split-mouth study. *J Periodontol, 72*(3), 296-302. doi: 10.1902/jop.2001.72.3.296

Paul, W., & Sharma, C. P. (2007). Effect of calcium, zinc and magnesium on the attachment and spreading of osteoblast like cells onto ceramic matrices. *J Mater Sci Mater Med, 18*(5), 699-703. doi: 10.1007/s10856-006-0005-1

Peltier, L. (1959). The Use of Plaster of Paris to Fill Large Defects in Bone *American Journal of Surgery, 97*.

Pietrzak, W. S., & Ronk, R. (2000). Calcium sulfate bone void filler: a review and a look ahead. *J Craniofac Surg, 11*(4), 327-333; discussion 334.

Rauh, J., Milan, F., Gunther, K. P., & Stiehler, M. (2011). Bioreactor systems for bone tissue engineering. *Tissue Eng Part B Rev, 17*(4), 263-280. doi: 10.1089/ten.TEB.2010.0612

Reilly, D. T., & Burstein, A. H. (1975). The elastic and ultimate properties of compact bone tissue. *J Biomech, 8*(6), 393-405.

Rho, J. Y., Kuhn-Spearing, L., & Zioupos, P. (1998). Mechanical properties and the hierarchical structure of bone. *Med Eng Phys, 20*(2), 92-102.

Serra, T. (2014). DEVELOPMENT OF 3D-PRINTED BIODEGRADABLE COMPOSITE SCAFFOLDS FOR TISSUE ENGINEERING APPLICATIONS. Universitat Politècnica de Catalunya.

Sharma, R., Bhargava, D., Rastogi, P., Yadav, M., Chandavarkar, V., Siddhartha, M., Caroli, P., Bansal, P. (2014). Stem Cells: An Update. *J Indian Acad Forensic Med., 36*(3).

Sidqui, M., Collin, P., Vitte, C., & Forest, N. (1995). Osteoblast adherence and resorption activity of isolated osteoclasts on calcium sulphate hemihydrate. *Biomaterials, 16*(17), 1327-1332.

Stock, U. A., & Vacanti, J. P. (2001). Tissue engineering: current state and prospects. *Annu Rev Med, 52*, 443-451. doi: 10.1146/annurev.med.52.1.443

Subia, B. K., J.; Kundu, S. C. . (2010). Biomaterial Scaffold Fabrication Techniques for Potential Tissue Engineering Applications. In D. Eberli (Ed.), *Tissue Engineering*.

Sun, W., Darling, A., Starly, B., & Nam, J. (2004). Computer-aided tissue engineering: overview, scope and challenges. *Biotechnol Appl Biochem, 39*(Pt 1), 29-47. doi: 10.1042/BA20030108

Suslu, A., Albayrak, A. Z., Urkmez, A. S., Bayir, E., & Cocen, U. (2014). Effect of surfactant types on the biocompatibility of electrospun HAp/PHBV composite nanofibers. *J Mater Sci Mater Med*. doi: 10.1007/s10856-014-5286-1

Tas, A. C. (2000). Synthesis of biomimetic Ca-hydroxyapatite powders at 37 degrees C in synthetic body fluids. *Biomaterials, 21*(14), 1429-1438.

Teoreanu, I., Preda, M., & Melinescu, A. (2008). Synthesis and characterization of hydroxyapatite by microwave heating using CaSO4.2H2O and Ca(OH)2 as calcium source. *J Mater Sci Mater Med, 19*(2), 517-523. doi: 10.1007/s10856-006-0038-5

Thomas, M. V., Puleo, D. A., & Al-Sabbagh, M. (2005). Calcium sulfate: a review. *J Long Term Eff Med Implants, 15*(6), 599-607.

Tiruvannamalai-Annamalai, R., Armant, D. R., & Matthew, H. W. (2014). A glycosaminoglycan based, modular tissue scaffold system for rapid assembly of perfusable, high cell density, engineered tissues. *PLoS One, 9*(1), e84287. doi: 10.1371/journal.pone.0084287

Upcraft, S. F., R. (2003). The rapid prototyping technologies. *Assembly Automation, 23*(4).

Utela, B., Storti, D., Anderson, R., & Ganter, M. (2008). A Review of Process Development Steps for New Material Systems in Three Dimentional Printing (3DP). *Journal of Manufacturing Processes, 10*(2).

Varghese, D., Deshpande, M., Xu, T., Kesari, P., Ohri, S., & Boland, T. (2005). Advances in tissue engineering: cell printing. *J Thorac Cardiovasc Surg, 129*(2), 470-472. doi: 10.1016/j.jtcvs.2004.06.050

Wang, M. (2004). *Biomaterials and Tissue Engineering* (D. Shi Ed.): Springer.

Wong, K. V., & Hernandez, A. (2012). A Review of Additive Manufacturing. *ISRN Mechanical Engineering, 2012*, 10.

Wu, H. D., Lee, S. Y., Poma, M., Wu, J. Y., Wang, D. C., & Yang, J. C. (2012). A Novel Resorbable α-Calcium Sulfate Hemihydrate/Amorphous Calcium Phosphate Bone Substitute for Dental Implantation Surgery. *Materials Science and Engineering C, 32*(3).

Xu, T. D., J. I.; Soriano, D. R.; Bhuyan, M.; Zhu, L.; Wang, K.; Yuan, Y. (2014). Principles of Bioprinting Technology. In G. Orlando (Ed.), *Regenerative Medicine Applications in Organ Transplantation*.

Yamada, N., Okano, T., Sakai, H., Karikusa, F., Sawasaki, Y., & Sakurai, Y. (1990). Thermoresponsive Polymeric Surfaces - Control of Attachment and Detachment of Cultured-Cells. *Makromolekulare Chemie-Rapid Communications, 11*(11), 571-576.

Yamaguchi, M. (1998). Role of Zinc in Bone Formation and Bone Resorption. *The Journal of Trace Elements in Experimental Medicine, 11*.

Yan, X., Huang, X., Yu, C., Deng, H., Wang, Y., Zhang, Z., . . . Zhao, D. (2006). The in-vitro bioactivity of mesoporous bioactive glasses. *Biomaterials, 27*(18), 3396-3403. doi: 10.1016/j.biomaterials.2006.01.043

Zhou, Z., Buchanan, F., Mitchell, C., & Dunne, N. (2014). Printability of calcium phosphate: calcium sulfate powders for the application of tissue engineered bone scaffolds using the 3D printing technique. *Mater Sci Eng C Mater Biol Appl, 38*, 1-10. doi: 10.1016/j.msec.2014.01.027

Zofkova, I., Nemcikova, P., & Matucha, P. (2013). Trace elements and bone health. *Clin Chem Lab Med, 51*(8), 1555-1561. doi: 10.1515/cclm-2012-0868

CIRRICULUM VITAE

Betül ALDEMİR

Erzurum, 1990

aldemirbetul@gmail.com

EDUCATION

(2016) M.Sc., İzmir Kâtip Çelebi Uni., Biomedical Technologies, GPA: 4.00/4.00

(2014) B.Sc., Anadolu Uni., International Relations and Affairs

(2013) B.Sc., Ege Uni., Bioengineering, GPA: 3.26/100

PROFESSIONAL EXPERIENCE AND REWARDS:

(2015) Ministry of National Education of the Republic of Turkey,
Post Graduated Scholarship

(2015) The Scientific and Technological Research Council of Turkey,
Project Scholarship

(2015) 19th National Biomedical Engineering Meeting,
Best Poster Award

(2012) IAESTE Internship Programme,
Summer Internship, Belgium

PUBLICATIONS, PRESENTATIONS AND PATENTS ON THE THESIS:

Presentations

- **Aldemir, B.,** Dikici, S., Karaman, O., Oflaz, H., (2015), **"Development, production and characterization of calcium sulfate based 3D scaffolds"**, 21st International Biomedical Science and Technology Symposium, BIOMED, October 22-24, Turkey (Poster)
- **Aldemir, B.,** Dikici, S.,Karaman, O., Oflaz, H., (2015), "**Development, 3D printing and characterization of calcium sulfate based scaffolds for bone tissue engineering",** 19. National Biomedical Engineering Meeting, BİYOMUT, November 5-6, Turkey (Poster)
- **Aldemir, B.**, Dikici, S., Öztürk, Ş., Karaman, O., Şendemir Ürkmez, A.i Oflaz, H. (2014), "**3D tissue scaffold printing on custom artificial bone applications**", Internationally Participated 7. National Biomechanics Congress, Turkey (Oral)

Publications

- **Aldemir, B.,** Dikici, S.,Karaman, O., Oflaz, H., (2015), "**Development, 3D printing and characterization of calcium sulfate based scaffolds for bone tissue engineering"**, 19th Biomedical Engineering Meeting (BIYOMUT), IEEE.
- **Aldemir, B.**, Dikici, S., Öztürk, Ş., Karaman, O., Şendemir Ürkmez, A., Oflaz, H. (2014), "**3D tissue scaffold printing on custom artificial bone applications**", Journal of Natural and Applied Science, 18 (3).

OTHER PUBLICATIONS, PRESENTATIONS AND PATENTS:

Presentatios

- **Aldemir, B.,** Oflaz, H., Karaman, O., (2015), "**Non-verbal description of science by medical illustration"**, 21st International Biomedical Science and Technology Symposium, BIOMED, October 22-24, Turkey (Oral)

- Dikici, S., **Aldemir, B.,** Gezgin, E., Başer,Ö., Şahin, S., Eser,H., Oflaz, H., (2015), **"Design of transvaginal uterus amputation device with 2-axis motion capacity and led illumination system for laparoscopic hysterectomies "**, 21st International Biomedical Science and Technology Symposium, BIOMED, October 22-24, Turkey (Poster)
- Dikici, S., Eser,H., **Aldemir, B.,** Gezgin, E., Başer,Ö., Şahin, S., Oflaz, H., (2015), "**Designing and prototyping of a new uterine manipulator which will overcome drawbacks of conventional uterine manipulators and assist laparoscopic hysterectomies"**, 19. National Biomedical Engineering Meeting, BİYOMUT, November 5-6, Turkey (Poster)
- Dikici, S., **Aldemir, B.**, Gezgin, E., Başer, Ö., Şahin, S., Eser, H., Ercan, U. K., Yılmaz, B., Kelekçi, S., Oflaz, H. (2014), **"Development of transvaginal uterus amputation device for laparoscopic hysterectomies in gynaecologic surgeries"**, Internationally Participated 7. National Biomechanics Congress, Turkey (Oral)

Publications

- Dikici, S., Eser,H., **Aldemir, B.,** Gezgin, E., Başer,Ö., Şahin, S., Oflaz, H., (2015), "**Designing and prototyping of a new uterine manipulator which will overcome drawbacks of conventional uterine manipulators and assist laparoscopic hysterectomies**", 19th Biomedical Engineering Meeting (BIYOMUT), IEEE.
- Dikici, S., **Aldemir, B.**, Gezgin, E., Başer, Ö., Şahin, S., Eser, H., Ercan, U. K., Yılmaz, B., Kelekçi, S., Oflaz, H. (2014), **"Development of transvaginal uterus amputation device for laparoscopic hysterectomies in gynaecologic surgeries"**, Journal of Natural and Applied Science, 18 (3).